Graduate School of Oceanography Faculty Publications

2012

Shelf-basin exchange times of Arctic surface waters estimated from ^{228}TH/^{228}Ra disequilibrium

M. Rutgers van der Loeff

P. Cai

See next page for additional authors

Authors

M. Rutgers van der Loeff, P. Cai, I. Stimac, D. Bauch, C. Hanfland, T. Roeske, and S. Bradley Moran

Shelf-basin exchange times of Arctic surface waters estimated from ^{228}Th/^{228}Ra disequilibrium

M. Rutgers van der Loeff,[1] P. Cai,[1,2] I. Stimac,[1] D. Bauch,[3] C. Hanfland,[1] T. Roeske,[1] and S. B. Moran[4]

[1]   The transpolar drift is strongly enriched in ^{228}Ra accumulated on the wide Arctic shelves with subsequent rapid offshore transport. We present new data of Polarstern expeditions to the central Arctic and to the Kara and Laptev seas. Because ^{226}Ra activities in Pacific waters are 30% higher than in Atlantic waters, we correct ^{226}Ra for the Pacific admixture when normalizing ^{228}Ra with ^{226}Ra. The use of ^{228}Ra decay as age marker critically depends on the constancy in space and time of the source activity, a condition that has not yet adequately been tested. While ^{228}Ra decays during transit over the central basin, ingrowth of ^{228}Th could provide an alternative age marker. The high ^{228}Th/^{228}Ra activity ratio (AR = 0.8–1.0) in the central basins is incompatible with a mixing model based on horizontal eddy diffusion. An advective model predicts that ^{228}Th grows to an equilibrium AR, the value of which depends on the scavenging regime. The low AR over the Lomonosov Ridge (AR = 0.5) can be due to either rapid transport (minimum age without scavenging 1.1 year) or enhanced scavenging. Suspended particulate matter load (derived from beam transmission and particulate ^{234}Th) and total ^{234}Th depletion data show that scavenging, although extremely low in the central Arctic, is enhanced over the Lomonosov Ridge, making an age of 3 years more likely. The combined data of ^{228}Ra decay and ^{228}Th ingrowth confirm the existence of a recirculating gyre in the surface water of the eastern Eurasian Basin with a river water residence time of at least 3 years.

Citation: Rutgers van der Loeff, M., P. Cai, I. Stimac, D. Bauch, C. Hanfland, T. Roeske, and S. B. Moran (2012), Shelf-basin exchange times of Arctic surface waters estimated from ^{228}Th/^{228}Ra disequilibrium, *J. Geophys. Res.*, *117*, C03024, doi:10.1029/2011JC007478.

1. Introduction

[2]   The Arctic Ocean comprises just 1% of World Ocean volume but receives 10% of World river discharge. Surface water with a large river water component and imprints from the wide shelf areas are carried across the central Arctic in the transpolar drift (TPD). With the rapid reduction of summer ice cover in the deep central Arctic major changes can be expected in primary production and biogeochemical cycles. How the central Arctic ecosystem will develop will strongly depend on the composition and circulation of the surface water. It is therefore important to quantify the rate and mode of surface water exchange between shelves and central basins. The circulation of surface waters in the central Arctic is not known as accurately as we know the ice

drift. It took the ice 2.9 years to carry Nansen's *Fram* from the Laptev Sea before leaving the Arctic at 80°N, but with 1979–2006 climatology this drift would on average have taken 3.7 years [*Pfirman et al.*, 2009]. The rapid drift of *Tara* in the years 2006–2008 (approximately 1.5 years, DAMOCLES Project) shows that the ice drift has lately accelerated, as is also documented by numerous buoys deployed in the ice and tracked by satellite (International Arctic Buoy Programme). The surface water residence time, which needs not be the same as that of the ice, was estimated by *Schlosser et al.* [1999] to be 2–5 years, but these authors mention that their method (tritium/^{3}He ages) gives a minimum estimate because of possible losses of ^{3}He to the atmosphere through leads in the ice. The residence time of freshwater in the Arctic is approximately 10 years [*Serreze et al.*, 2006].

[3]   The natural radionuclide ^{228}Ra is a powerful tracer for shelf inputs to the open ocean [*Moore et al.*, 1986] and is particularly well suited for such studies in the Arctic Ocean, which comprises 25% of the World shelf areas. Earlier ^{228}Ra measurements from 1991 [*Rutgers van der Loeff et al.*, 1995] and 1994 [*Smith et al.*, 2003] showed high surface water ^{228}Ra activities in the TPD. *Kadko and Muench* [2005] confirmed low ^{228}Ra/^{226}Ra in the Beaufort Gyre due to decay during the long residence time in this basin.

[1]Alfred Wegener Institute for Polar and Marine Research, Bremerhaven, Germany.
[2]State Key Laboratory of Marine Environmental Science, Xiamen University, Xiamen, China.
[3]Leibniz Institute of Marine Sciences at University Kiel (IFM-GEOMAR), Kiel, Germany.
[4]Graduate School of Oceanography, University of Rhode Island, Narragansett, Rhode Island, USA.

Table 1. Station Date, Depth, and Position During Polarstern Expedition ARK XI/1

Station ARK-XI/1-	Date	Depth	Latitude (°N)	Longitude (°E)
2	19-07-1995	151	77.523	97.065
3	22-07-1995	1982	77.704	125.910
4	24-07-1995	54	78.010	144.889
6	25-07-1995	96	78.978	147.346
7	26-07-1995	210	79.455	148.108
9	29-07-1995	75	78.655	144.122
10	30-07-1995	50	78.002	140.003
12	31-07-1995	45	77.252	135.002
16	31-07-1995	51	76.002	130.012
18	01-08-1995	95	77.597	130.008
19	01-08-1995	264	77.622	130.047
21	02-08-1995	1180	77.857	130.030
23	03-08-1995	2354	78.158	129.973
24A	05-08-1995	3263	79.314	131.518
25	07-08-1995	2670	81.135	105.559
29	10-08-1995	2222	80.900	104.742
31	11-08-1995	1588	80.780	103.440
33	12-08-1995	253	80.427	102.017
40	15-08-1995	1780	78.531	133.979
42	16-08-1995	2176	78.698	134.608
44	17-08-1995	2679	79.137	135.007
45	18-08-1995	3424	79.999	134.961
47	20-08-1995	3909	80.915	131.155
49	22-08-1995	2650	81.053	136.565
51	23-08-1995	1742	81.071	138.928
52	24-08-1995	1215	81.160	140.155
56	26-08-1995	2428	81.177	147.399
60	28-08-1995	1778	80.341	149.975
62	29-08-1995	1063	80.081	149.842
65	30-08-1995	234	79.515	148.239
71	01-09-1995	604	78.341	135.075
73	02-09-1995	107	78.247	135.392
80	06-09-1995	1244	78.768	112.732
84	07-09-1995	95	77.895	113.718
89	09-09-1995	2721	82.343	92.848
91	10-09-1995	1079	82.072	91.038
94	10-09-1995	93	81.820	90.768

Hansell et al. [2004] and *Letscher et al.* [2011] used this decay to derive decomposition rates of dissolved organic carbon. *Kadko and Aagaard* [2009] derived water mass ages of halocline waters using submarine-collected samples. This use of the decay of ^{228}Ra to derive the time since a water parcel left the shelf is critically dependent on the assumption that the ^{228}Ra activity of waters, when they leave contact with the shelf, is known and constant over time and space. This has not been tested yet. In fact, there are indications that there are differences between individual shelf areas [*Rutgers van der Loeff et al.*, 2003]. Indications of a systematic difference between Eurasian and American shelf concentrations [*Smith et al.*, 2003] were not supported by *Kadko and Muench* [2005], who argue that their data from the Chukchi are in accord with published distributions in the Eurasian Arctic.

[4] The general circulation of surface waters in the Arctic Ocean is characterized by an anticyclonic (clockwise) circulation in the Beaufort Gyre and a cyclonic circulation in the Eurasian Basin. The two systems meet in the TPD [*Pfirman et al.*, 1997; *Rudels*, 2009] which forms the transition between waters of Pacific and Atlantic origin. Depending on the Arctic Oscillation the general circulation changes between periods with stronger cyclonic or anticyclonic character [*Proshutinsky and Johnson*, 1997]. In the

1990s, a strong change toward cyclonic circulation weakened the Beaufort Gyre and the Atlantic/Pacific front shifted from approximately the Lomonosov to the Alpha/Mendeleev Ridges [*McLaughlin et al.*, 1996; *Ekwurzel et al.*, 2001], which resulted in a shift in the geographic positions of maximum ^{228}Ra concentrations [*Smith et al.*, 2003]. Such changes in surface circulation likely change the residence time of water over the shelves and may therefore also have changed the accumulated ^{228}Ra activities. While ^{228}Ra may thus be a useful tracer for the variability in the outflow of shelf water from the Laptev Sea [*Smith et al.*, 2003], the calculation of surface water age from ^{228}Ra activities becomes questionable. It is therefore desirable to have additional tracers of the transit time of water in the TPD.

[5] The ingrowth of ^{228}Th into its parent ^{228}Ra could serve that purpose. We know from studies of ^{234}Th that thorium is effectively removed on the shelves (Barents Sea [*Coppola et al.*, 2002; *Rutgers van der Loeff et al.*, 2002], Chukchi Sea [*Moran et al.*, 1997; *Moran et al.*, 2005; *Lalande et al.*, 2007; *Lepore et al.*, 2007], Beaufort Sea [*Moran and Smith*, 2000], Laptev Sea [*Cai et al.*, 2010]). These high thorium scavenging rates also cause ^{228}Th to be depleted with respect to ^{228}Ra [*Trimble et al.*, 2004; *Lepore and Moran*, 2007]. In the Canada Basin thorium scavenging rates decrease northward [*Moran et al.*, 1997; *Trimble et al.*, 2004; *Trimble and Baskaran*, 2005] and reach very low values on the Alpha Ridge in the central Arctic [*Bacon et al.*, 1989]. Indeed, in large areas of the central Arctic, scavenging rates are extremely low [*Cai et al.*, 2010]. Thus, when ^{228}Th-depleted shelf waters are carried along in the transpolar drift and flow into the low-scavenging regime of the central Arctic, it can be expected that ^{228}Th grows into equilibrium with its parent ^{228}Ra. Here we investigate to what extent the ^{228}Th/^{228}Ra ratio in Arctic surface waters can be used to derive the age of a surface water parcel since it left the high-scavenging regime on the shelf.

2. Methods

2.1. ARK XI/1 (1995)

[6] During the German-Russian expedition with R/V *Polarstern* to the Laptev Sea, 7 July to 20 September 1995 [*Rachor*, 1997], seawater samples of about 40 L were collected at 37 stations (Table 1) with the 24 × 12 L Rosette sampler. After filtration, a solution of barium chloride was added to the samples to coprecipitate radium with BaSO$_4$. At 16 of these stations the samples had previously been acidified, spiked with Fe and ^{230}Th and neutralized with ammonia to isolate Th isotopes on a Fe(OH)$_3$ precipitate. This coprecipitation does not remove Ra [*Li et al.*, 1980]. The BaSO$_4$ precipitates were dried and put in small tubes. Radium activities were determined by gamma spectrometry at the home laboratory.

[7] The freshwater components were calculated using the δ^{18}O data of *Frank* [1996] and the three-component (Atlantic water, meteoric water and ice melt) mixing model of *Östlund and Hut* [1984] with end-member compositions according to *Ekwurzel et al.* [2001].

2.2. ARK XXII/2 (2007)

[8] Surface water samples (150–300 L) were collected during Polarstern Expedition ARK XXII/2, 29 July to
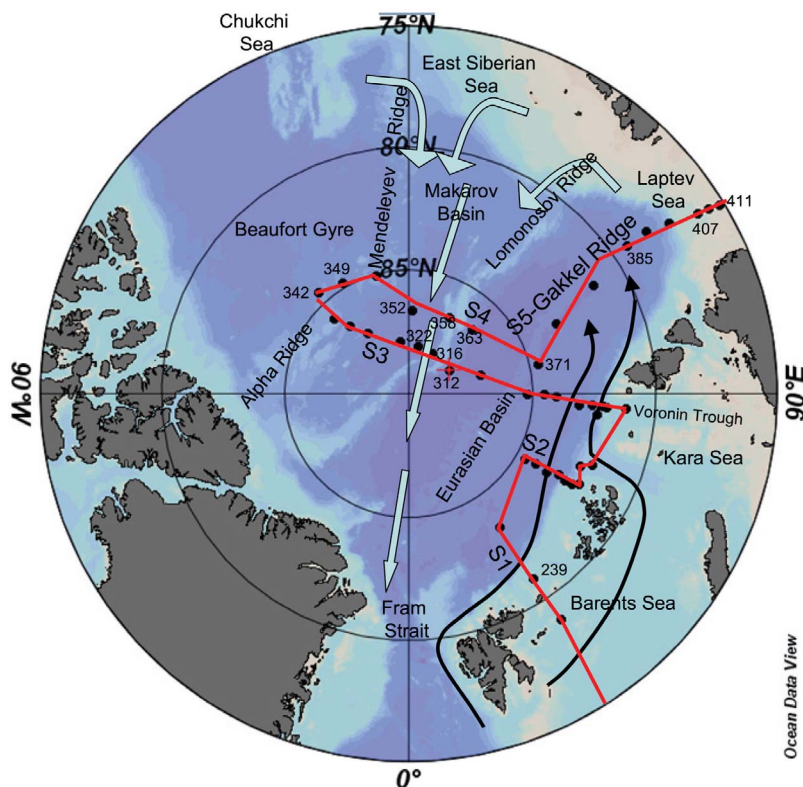
Figure 1. Cruise track (red lines) with sections (S1–S5) and stations sampled during Polarstern ARK XXII/2 with Atlantic inflow in the Fram Strait and Barents Sea branches (black lines) and approximate pathway of the TPD (arrows).

7 October 2007 [*Schauer*, 2008] (Figure 1). Samples from the seawater intake at 7 m depth were filtered over 1 μm polypropylene cartridges, passed over MnO$_2$ fibre at a flow rate of at most 1 L/min to obtain a Ra extraction efficiency of at least 97% [*Moore*, 2008] and counted for ^{224}Ra with delayed coincidence scintillation counting [*Moore and Arnold*, 1996]. For the calculation of counts due to ^{224}Ra we used the chance coincidence correction, not the alternative procedure based on total counts [*Moore*, 2008]. The expected error is 8–14% [*Garcia-Solsona et al.*, 2008]. The same procedure can in principle be used to determine ^{227}Ac through ^{223}Ra [*Geibert et al.*, 2008] but count rates were influenced by the high count rates of ^{224}Ra and buildup of ^{222}Rn and activities were low and are not reported here. In the home laboratory, Ra was leached from the fibre [*Elsinger et al.*, 1982], coprecipitated as BaSO$_4$ [*Cutter et al.*, 2010] and counted with gamma spectroscopy for ^{226}Ra and ^{228}Ra [*Moore*, 1984].

[9] Beyond the reach of the unsupported ^{224}Ra from its shelf source [cf. *Kadko et al.*, 2008], ^{224}Ra must be in equilibrium with its parent ^{228}Th. That means that in offshore regions, the delayed coincidence technique provides an indirect technique to monitor ^{228}Th. In studies where excess ^{224}Ra is measured, the ^{224}Ra is recounted after the decay of the first generation ^{224}Ra in order to determine ^{228}Th-supported ^{224}Ra. We have recounted the samples after two half lives and found generally a 20% reduction in count rate. Because we observed this difference even in the central Arctic where an excess activity is not possible at large distance to any potential source, we interpret this not as

indication of real in situ ^{224}Ra excess, but rather as an apparent excess due to insufficient collection of ^{228}Th. This could be due either to filtration, which removes the particulate ^{228}Th, or to nonquantitative adsorption of Th to the Mn fibres. We have also considered the possibility that the seawater inlet of Polarstern had accumulated ^{228}Th during previous expeditions, which would then serve as a continuous source of ^{224}Ra as has been observed on other ships. The fact that we were able to measure low ^{224}Ra in the Atlantic inflow makes it unlikely that such a contamination was a significant contribution to the observed excess ^{224}Ra. We therefore consider the ^{224}Ra activities derived from the initial count rates to represent the total ^{228}Th activity and in this paper will report them as ^{228}Th. In shelf regions this procedure might overestimate ^{228}Th if a significant contribution of unsupported ^{224}Ra were present. On stations 407 and 411 on the Laptev shelf we deployed in situ pumps and measured ^{228}Th with the double-MnO$_2$ cartridge technique [*Baskaran et al.*, 1993] at four horizons. Dissolved ^{228}Th was 13 $\pm$ 8 dpm/m^3, particulate ^{228}Th was 1–2 dpm/m^3 compared with a ^{224}Ra activity of 21 $\pm$ 15 dpm/m^3 measured with RaDeCC in discrete water samples collected at these stations (Table 2), resulting in an average ^{224}Ra/^{228}Th ratio of 1.45. In five cases where we measured ^{224}Ra (RaDeCC) and ^{228}Th (in situ pumps) at the same station and depth, ^{224}Ra/^{228}Th AR ranged from 0.3 to 2.1 (Table 2). As values of this AR below 1 are unlikely, we explain the wide range by inhomogeneity while the two isotopes were sampled 3 h apart with different gear. We conclude that in individual

Table 2. In situ Pump (ISP) and RaDeCC (Rosette Sampling) Data of ^{228}Th, ^{228}Ra, and ^{224}Ra From the Laptev Shelf

Station	Depth (m) ISP	^{228}/^{226}Ra ISP	^{226}Ra (dpm/m³) 20 L	^{228}Ra (dpm/m³) ISP	^{228}Th (dpm/m³) Dissolved ISP	^{228}Th (dpm/m³) Part ISP	^{228}Th (dpm/m³) Total ISP	^{228}Th/^{228}Ra ISP	Depth (m) RADECC	^{228}/^{226}Ra RADECC	^{224}Ra (dpm/m³) RADECC	^{228}Ra (dpm/m³) RADECC	^{224}Ra/^{228}Ra RADECC	^{224}Ra/^{228}Th
385	7	0.50 ± 0.02	81.1 ± 4.8	41 ± 3					7	0.46 ± 0.02	18.0 ± 1.8	31.1 ± 1.4	0.58 ± 0.06	
407	7	1.27 ± 0.05	71.8 ± 4.1	91 ± 6	7	1.4[b]	8	0.09	7	1.16 ± 0.03	16.7 ± 1.7	56.2 ± 1.5	0.30 ± 0.03	2.0
407	15	3.91 ± 0.18	75[a] ± 5	293 ± 24	5	0.75	6	0.02						
407	30	1.29 ± 0.05	75[a] ± 5	97 ± 8	29	1.75	31	0.32	30	0.85 ± 0.02	10.9 ± 1.1	75.7 ± 2.3	0.14 ± 0.02	0.4
407	50	0.44 ± 0.02	75[a] ± 5	33 ± 3	7	2.38	9	0.29	65	0.85 ± 0.02	21.7 ± 2.2	81.5 ± 2.3	0.27 ± 0.03	2.3
411	7	1.35 ± 0.13	79.6 ± 4.2	107 ± 12	10	1.4[b]	11	0.11	7	1.02 ± 0.04	9.7 ± 1.0	34.1 ± 1.5	0.28 ± 0.03	0.9
411	15	1.51 ± 0.15	75[a] ± 5	113 ± 14	9	0.33	9	0.08						
411	25	1.86 ± 0.19	75[a] ± 5	140 ± 17	20	1.65	22	0.15	25	1.91 ± 0.03	47.0 ± 4.7	247.1 ± 3.2	0.19 ± 0.02	2.2
411	35	1.83 ± 0.19	75[a] ± 5	137 ± 17	19	1.4[b]	20	0.15						
Shelf average (Sta 407–411)					13.3		14.6	0.15			21.2		0.24	1.5
SD					8.5		8.7	0.10			15.2		0.07	0.9

[a]Not measured, average of shelf samples in Figure 2 (top).
[b]Not measured, average of other particulate samples.

shelf water samples the measured ^{224}Ra/^{228}Ra may overestimate in situ ^{228}Th/^{228}Ra by up to a factor of 2 (Table 2).

[10] The freshwater and Pacific components for ARK XXII/2 (2007) were calculated using δ^{18}O and nutrient data following *Bauch et al.* [2011], using the N/P characteristics of Atlantic and Pacific waters following *Jones et al.* [1998] and *Yamamoto-Kawai et al.* [2008]. For further details on calculations and errors refer to *Bauch et al.* [2011]. For stations where the calculated Pacific component f_P was negative and for stations on the Laptev shelf (Station 385 and beyond) f_P was set to zero.

[11] Some depth profiles were obtained on the Laptev shelf with in situ pumps equipped with size-fractionated filters and twin MnO_2-coated cartridges. Cartridges were leached with a Soxhlet system and Ra was precipitated as $BaSO_4$ and gamma counted as the other samples. The Th fractions of the Soxhlet leaches and of the filter digest solutions [*Cai et al.*, 2010] were analyzed for ^{228}Th with alpha spectrometry.

[12] Particulate ^{234}Th was monitored with a semi-automated filtration apparatus [*Rutgers van der Loeff et al.*, 2011, 2006] set to filter approximately every 4 h 4.9 L of surface water from the ship's seawater intake over 25 mm QMA filters that were subsequently dried and counted for beta activity. Graphics were produced with the ODV software package (R. Schlitzer, Ocean Data View, 2010, http://odv.awi.de). All data of ^{228}Th and Ra isotopes are presented in Tables 3 and 4 and are available in the database PANGAEA (doi:10.1594/PANGAEA.772682). On this GEOTRACES expedition a wide spectrum of other trace elements and isotopes was measured (see http://www.bodc.ac.uk/geotraces/data/inventories/arkxxii_2/).

3. Results

3.1. Radium-226

[13] In many studies on ^{228}Ra in the open ocean the long-lived isotope ^{226}Ra has been used as a yield tracer determined either in discrete samples [*Smith et al.*, 2003; *Rutgers van der Loeff et al.*, 2003] or derived from published relationships between ^{226}Ra, salinity and silicate [*Broecker et al.*, 1976; *Moore and Smith*, 1986; *Rutgers van der Loeff et al.*, 1995].

[14] A plot of ^{226}Ra activity against f_r (Figure 2, top) shows the major features of ^{226}Ra in surface waters in the Arctic Ocean: First, ^{226}Ra activities in all samples with a significant component of Pacific water are approx 30% higher than in the Eurasian Basin (Figure 2 (top) and map in Figure 3). *Moore and Smith* [1986] had already observed that the surface water concentration of ^{226}Ra at the Cesar Ice camp station (85°50′N, 108°50′W: 107 dpm/m³) was somewhat higher than reported North Atlantic and Greenland Sea surface values corrected to 35 ‰ salinity and zero dissolved silicate (68–73 dpm/m³ [*Broecker et al.*, 1976]); (70 ± 2 to 77 ± 2 for TTO samples N of 70°N [*Key et al.*, 1992]). *Moore and Smith* [1986] argued that the Cesar values were closer to North Pacific surface values from the GEOSECS program (96 dpm/m³ at 32 μM Si [*Chung and Craig*, 1980]). Similarly high ^{226}Ra activities (113.8, 113.8, 109.7 dpm/m³) were observed in surface waters of the deep (>1000 m) Canada Basin by *Smith et al.* [2003] but data published for the Chukchi and Beaufort shelf areas

Table 3. Sampling Depth, Potential Temperature, Salinity, Fraction of River Water, and ^{226}Ra and ^{228}Ra Activity With Propagated 1 σ Counting Errors During ARK XI/1 (Data Available on www.pangaea.de)

Station ARK-XI/1-	Depth (m)	Pot Temp (°C)	Salinity	f_r (%)	^{226}Ra (dpm/m^3)	^{228}Ra (dpm/m^3)
2	5	−1.19	31.38	11.24	80.0 ± 6.2	−7.9 ± 11.5
2	51	−1.64	33.88	4.74	91.8 ± 3.0	58.2 ± 5.4
2	126	−1.29	34.26	2.72	105.2 ± 2.9	45.7 ± 4.9
3	5				88.7 ± 2.3	58.8 ± 4.1
3	30				93.9 ± 2.5	53.8 ± 4.4
3	50				93.2 ± 2.8	44.5 ± 4.7
3	251				100.2 ± 2.4	8.9 ± 3.5
3	1500				113.6 ± 1.6	8.6 ± 2.2
4	5	0.13	30.88	15.53	105.3 ± 6.0	180.0 ± 13.3
4	30	−1.75	33.07	13.29	111.0 ± 4.7	167.8 ± 9.9
6	5	−1.77	33.39	8.44	93.3 ± 6.0	84.7 ± 11.5
7	17	−1.76	33.23	7.58	100.9 ± 4.9	55.1 ± 8.3
7	50			3.46	102.1 ± 3.7	54.1 ± 6.3
7	100	−0.8	34.33	2.16	100.2 ± 5.1	44.7 ± 8.5
7	150	−0.8	34.33	2.16	109.5 ± 3.9	31.8 ± 5.9
7	205	0.83	34.75	0.59	107.7 ± 3.8	22.3 ± 5.9
9	5	−1.71	32.87	12.13	96.5 ± 5.1	151.5 ± 10.7
9	50	−1.8	33.44	9.30	101.2 ± 6.1	102.3 ± 11.7
10	5	0.59	32.39	11.27	92.6 ± 5.6	89.4 ± 10.3
10	40	−1.67	33.08	11.09	98.0 ± 5.1	110.8 ± 9.8
12	5	4.12	29.91	13.92	66.6 ± 5.9	87.7 ± 12.0
12	31	−1.69	32.75	10.66	83.8 ± 6.3	78.5 ± 12.0
16	5	2.36	28.78	18.11	77.0 ± 3.9	72.8 ± 7.4
16	40	−1.37	33.66	4.92	103.3 ± 5.6	88.0 ± 10.5
18	5	2.46	28.67	16.38	75.4 ± 7.4	112.0 ± 15.2
19	4	−1.42	30.95	12.42	84.7 ± 4.4	58.1 ± 7.4
19	39	−0.98	34.21	2.80	95.1 ± 4.8	52.6 ± 8.3
19	99	−0.97	34.31	2.29	108.3 ± 5.3	51.1 ± 8.7
19	200	−0.83	34.35	2.24	99.9 ± 5.7	37.7 ± 9.4
19	250	−0.82	34.35	2.14	95.9 ± 4.8	44.7 ± 8.1
21	5	−0.98	29.81	14.31	70.4 ± 4.7	56.9 ± 8.7
21	51	−1.68	33.6	4.66	73.1 ± 4.4	43.0 ± 8.1
21	250	1.55	34.83	0.29	83.7 ± 3.4	14.3 ± 5.2
21	1048	−0.01	34.88	0.29	94.5 ± 3.5	25.0 ± 5.5
23	5	−1.14	30.31	14.12	67.6 ± 3.7	52.4 ± 6.7
23	51	−1.84	33.73	4.67	76.7 ± 4.2	43.8 ± 7.1
23	250	1.97	34.89	0.19	75.5 ± 1.7	8.6 ± 2.6
23	1198	−0.31	34.9	0.35	82.9 ± 2.5	24.4 ± 3.9
23	2198	−0.78	34.92	0.09	96.5 ± 3.1	15.1 ± 4.6
23	2329	−0.79	34.93	0.15	93.3 ± 3.4	12.5 ± 4.8
24A	10				72.7 ± 5.7	51.7 ± 11.0
24A	50	−1.8	33.24	5.95	79.9 ± 3.7	30.9 ± 6.3
24A	250	1.88	34.88	0.29	91.7 ± 2.8	10.6 ± 4.2
24A	1151				97.3 ± 3.5	12.5 ± 5.5
24A	3250	−0.74	34.94	−0.06	113.1 ± 3.6	8.3 ± 4.9
25	10				98.3 ± 3.2	34.8 ± 5.2
25	51				91.2 ± 2.4	24.6 ± 3.8
25	250				97.3 ± 2.5	5.9 ± 3.6
25	547	0.77	34.87	0.24	85.1 ± 1.9	9.1 ± 2.9
25	800	0.22	34.91	0.30	91.7 ± 2.8	6.5 ± 4.2
25	2650	−0.78	34.94	0.20	108.5 ± 2.9	8.3 ± 4.3
29	615	0.33	34.87	0.45	91.7 ± 2.2	14.2 ± 3.2
31	11	−1.28	32.53	3.62	84.0 ± 3.7	35.7 ± 6.0
31	50	−1.7	34.24	1.99	97.0 ± 2.4	29.9 ± 3.8
31	228	1.35	34.8	0.27	97.2 ± 3.1	17.0 ± 4.4
31	800	−0.6	34.75	0.55	98.4 ± 2.9	30.6 ± 4.6
31	1400	−0.49	34.8	0.54	98.8 ± 2.2	20.0 ± 3.4
31	1567	−0.53	34.81	0.45	102.0 ± 2.6	21.0 ± 3.9
33	11	−1.52	33.53	2.52	83.2 ± 3.1	32.1 ± 5.0
33	43	−1.59	34.39	1.64	100.0 ± 3.9	26.8 ± 6.1
33	111	0.39	34.74	0.74	97.9 ± 3.4	25.0 ± 5.2
33	203	−0.55	34.72	0.88	97.2 ± 2.4	23.8 ± 3.8
33	238	−0.33	34.75	0.96	91.5 ± 2.9	20.2 ± 4.3
40	5				79.0 ± 3.3	52.3 ± 5.5
40	50	−1.81	33.62	4.57	85.6 ± 3.5	30.7 ± 5.3
40	282	1.93	34.87	0.35	90.5 ± 2.1	7.6 ± 3.1
40	588	0.56	34.86	0.48	96.6 ± 2.8	12.8 ± 4.1
40	1759	−0.63	34.91	0.16	101.9 ± 3.1	10.6 ± 4.7
42	5				70.5 ± 2.7	48.0 ± 4.8
42	52				92.9 ± 3.7	38.9 ± 5.9

Table 3. (continued)

Station ARK-XI/1-	Depth (m)	Pot Temp (°C)	Salinity	f_r (%)	^{226}Ra (dpm/m^3)	^{228}Ra (dpm/m^3)
42	268				90.4 ± 1.8	2.6 ± 2.6
42	1529	−0.57	34.9	0.25	96.3 ± 3.0	11.5 ± 4.6
42	2138				94.7 ± 2.5	9.6 ± 3.6
44	11	−1.62	30.76	13.08	78.7 ± 3.0	53.2 ± 5.3
44	51	−1.71	33.28	5.94	83.6 ± 3.0	34.9 ± 4.9
44	256	1.85	34.87	0.34	96.4 ± 2.2	7.5 ± 3.0
44	569	0.75	34.87	0.24	88.8 ± 2.7	9.4 ± 4.2
44	2864	−0.77	34.93	0.20	108.7 ± 3.2	5.1 ± 4.6
45	5	−1.6	30.42	13.62	73.6 ± 3.5	62.5 ± 6.6
45	254	1.79	34.87	0.45	81.2 ± 2.2	11.9 ± 3.3
45	1100	−0.38	34.89	0.35	85.9 ± 2.3	9.7 ± 3.3
45	3407	−0.72	34.94	0.25	92.8 ± 1.6	6.4 ± 2.3
47	9	−1.61	31.2	11.44	69.6 ± 4.4	34.0 ± 7.9
47	700	0.07	34.88	0.39	92.6 ± 2.7	18.5 ± 4.1
47	1999	−0.75	34.92	0.15	104.2 ± 3.0	6.5 ± 4.2
47	3914	−0.69	34.94	0.05	106.1 ± 1.9	10.5 ± 2.6
49	9	−1.6	30.43	12.45	75.6 ± 3.6	59.9 ± 6.3
49	261				79.9 ± 2.4	15.3 ± 3.6
49	751	−0.08	34.86	0.09	81.7 ± 2.6	24.9 ± 4.0
49	2381				99.7 ± 2.8	9.2 ± 4.0
51	5	−1.66	31.12	11.23	75.1 ± 4.4	48.8 ± 7.5
51	249	1.43	34.86	0.49	79.0 ± 1.8	12.7 ± 2.8
51	745	0.11	34.85	0.34	76.1 ± 2.6	21.8 ± 4.1
51	1667				103.1 ± 2.6	10.1 ± 3.7
51	1725	−0.57	34.92	0.10	103.5 ± 2.9	9.7 ± 4.2
52	5	−1.66	31.21	11.64	68.2 ± 3.9	39.8 ± 6.9
52	502	0.6	34.86	0.44	79.5 ± 2.0	17.4 ± 3.0
52	1182	−0.38	34.89	0.30	89.0 ± 2.2	19.8 ± 3.3
56	13	−1.71	31.97	9.50	76.0 ± 4.1	41.8 ± 7.2
56	257	1.41	34.84	0.49	87.7 ± 2.8	12.6 ± 4.3
56	637	0.29	34.86	0.25	79.3 ± 2.3	8.3 ± 3.5
56	1500	−0.44	34.91	0.25	97.9 ± 2.2	−2.2 ± 3.1
56	2413	−0.38	34.95	0.10	128.1 ± 2.8	3.4 ± 3.6
60	5	−1.76	33.01	8.46	79.4 ± 3.1	25.3 ± 5.0
60	50	−1.73	33.25	6.81	74.0 ± 7.8	19.5 ± 14.8
60	750	0.07	34.86	0.44	95.7 ± 2.3	14.5 ± 3.2
60	1676	−0.54	34.92	0.25	113.8 ± 2.2	7.0 ± 3.0
60	1745	−0.43	34.94	0.24	149.2 ± 2.2	9.8 ± 2.8
62	10	−1.69	32.19	8.17	87.7 ± 2.7	35.6 ± 4.5
62	51	−1.74	33.24	5.51	90.7 ± 3.3	27.0 ± 5.2
62	251	1.54	34.85	0.15	94.0 ± 2.7	9.6 ± 3.9
62	500	0.43	34.84	0.44	84.2 ± 2.4	12.0 ± 3.6
62	1049	−0.18	34.88	0.15	75.1 ± 1.8	16.1 ± 2.8
65	9	−1.71	32.28	8.22	85.1 ± 2.8	41.4 ± 4.7
65	50	−1.79	33.44	7.32	97.5 ± 2.8	53.5 ± 4.5
65	100	−1	34.2	2.22	88.7 ± 3.1	35.8 ± 5.0
65	179	0.78	34.66	0.46	92.3 ± 2.9	15.2 ± 4.4
65	217	1.08	34.72	0.55	97.1 ± 2.2	21.6 ± 3.4
71	10	0.58	28.9	15.04	65.4 ± 2.3	44.7 ± 4.1
71	272	1.77	34.85	0.24	79.2 ± 2.6	5.7 ± 3.9
71	585	0.6	34.86	0.29	81.3 ± 2.4	11.0 ± 3.7
73	10	0.16	28.83	15.18	56.7 ± 3.5	37.7 ± 6.4
73	30	−1.49	33.51	5.80	74.0 ± 2.8	33.9 ± 4.7
73	92	−1.3	34.09	3.45	85.6 ± 3.3	24.6 ± 5.1
80	10	1.3	32.42	7.23	47.6 ± 3.0	32.5 ± 5.5
80	250	1.17	34.85	0.55	81.2 ± 2.1	13.4 ± 3.2
80	318	0.92	34.84	0.60	88.6 ± 2.8	14.5 ± 4.1
80	920	−0.52	34.84	0.44	82.1 ± 2.6	20.8 ± 4.0
80	1212	−0.43	34.88	0.40	88.7 ± 2.8	21.9 ± 4.4
84	9	−0.13	30.16	11.06	54.5 ± 3.2	37.9 ± 6.1
84	76	−1.38	34.02	3.70	86.4 ± 3.5	43.6 ± 5.8
89	5				44.9 ± 3.7	10.6 ± 6.4
89	230				75.0 ± 2.5	7.7 ± 3.8
89	902	−0.43	34.87	0.25	86.9 ± 2.6	15.3 ± 4.0
89	2694	−0.78	34.93	0.00	109.8 ± 2.5	9.2 ± 3.3
91	5				48.4 ± 2.7	23.8 ± 4.8
91	268	0.77	34.82	0.64	82.7 ± 2.4	17.9 ± 3.7
91	500	−0.33	34.85	0.64	85.3 ± 2.8	22.8 ± 4.6
91	1110	−0.55	34.86	0.44	91.8 ± 2.9	32.0 ± 4.7
94	11	−1.67	32.19	3.69	79.6 ± 4.8	35.1 ± 8.4
94	76	−1.36	34.52	1.24	82.1 ± 1.6	36.8 ± 2.7

Table 4. Station Number, Date of Sampling, Bottom Depth, Position, Sampling Depth, Temperature, Salinity, Light Transmission, Fraction of Pacific and of River Water, Sample Volume, ^{224}Ra (RaDeCC), ^{226}Ra and ^{228}Ra Activity, ^{228}Ra/^{226}Ra Ratio and ^{228}Ra/^{226}Ra* Ratio (Corrected for Pacific ^{226}Ra Component) and the ^{228}Th/^{228}Ra Ratio (From ^{224}Ra/^{228}Ra) With Propagated 1 σ Counting Errors During ARK XXII/2 (Data Available on www.pangaea.de)

Station	Date	Bottom Depth (m)	Latitude (°N)	Longitude (°E)	Depth (m)	Temperature (°C)	Salinity	Transmission (%)	f_P (%)	f_r (‰)	Volume (L)	^{224}Ra (dpm m^{-3})	^{226}Ra (dpm m^{-3})	^{228}Ra (dpm m^{-3})	^{228}Ra/^{226}Ra	^{228}Ra/^{226}Ra*	^{228}Th/^{228}Ra
237	2007-07-31	276	78.997	33.995	7	−1.52	34.231		4.3	0.9	295	5.6 ± 0.6	68.9 ± 0.7	20.1 ± 1.1	0.29 ± 0.01	0.29	0.28 ± 0.03
239	2007-08-01	222	80.995	33.996	7	−0.97	32.664		0.0	1.1	295	2.7 ± 0.3	54.6 ± 0.6	19.1 ± 1.0	0.35 ± 0.01	0.35	0.14 ± 0.02
257	2007-08-05	3958	83.497	34.047	7	−1.57	33.385	91.46	0.0	0.0	292	12.8 ± 1.3	71.9 ± 0.8	16.1 ± 1.1	0.22 ± 0.01	0.22	0.79 ± 0.10
261	2007-08-11	3854	84.645	60.934	7	−1.59	33.382		0.5	2.7	293	17.2 ± 1.7	71.8 ± 1.1	17.2 ± 1.5	0.24 ± 0.02	0.24	1.00 ± 0.13
263	2007-08-11	3702	84.173	60.999	7	−1.62	33.780	91.46	2.2	1.1	295	11.0 ± 1.1	68.7 ± 0.6	13.0 ± 0.9	0.19 ± 0.01	0.19	0.85 ± 0.10
264	2007-08-12	3512	83.654	60.425	7	−1.65	33.555	91.33	4.8	0.0	292	10.2 ± 1.0	75.3 ± 0.6	15.9 ± 0.8	0.21 ± 0.01	0.21	0.64 ± 0.07
266	2007-08-13	3040	83.138	61.741	7	−1.64	33.314		0.0	1.8	295	8.1 ± 0.8	74.3 ± 0.9	19.2 ± 1.3	0.26 ± 0.01	0.26	0.42 ± 0.05
268	2007-08-14	1575	82.806	60.797	7	−1.61	32.856		0.0	2.1	295	6.6 ± 0.7	70.2 ± 0.6	16.1 ± 0.9	0.23 ± 0.01	0.23	0.41 ± 0.05
271	2007-08-15	327	82.501	60.783	7	−1.53	32.945		0.0	2.3	295	8.0 ± 0.8	70.6 ± 0.6	15.6 ± 0.9	0.22 ± 0.01	0.22	0.51 ± 0.06
272	2007-08-15	231	82.252	61.996	7	−1.53	32.945		0.0		295	8.2 ± 0.8	69.0 ± 0.6	14.7 ± 0.8	0.21 ± 0.01	0.21	0.56 ± 0.06
274	2007-08-16	1174	82.521	67.110	7	−1.37	33.745	88.37	0.3	1.1	295	8.5 ± 1.0	72.7 ± 0.7	16.2 ± 0.9	0.22 ± 0.01	0.22	0.53 ± 0.06
276	2007-08-17	680	82.083	68.960	7	−1.69	32.904	84.88	0.0	2.8	295	9.8 ± 1.0	74.9 ± 0.6	24.7 ± 0.8	0.33 ± 0.01	0.33	0.39 ± 0.04
277	2007-08-18	1526	82.392	83.832	7	−1.66	32.640	88.04	0.0	4.4	295	3.6 ± 0.4	60.4 ± 0.8	29.0 ± 1.5	0.48 ± 0.02	0.48	0.12 ± 0.01
279	2007-08-19	325	81.230	86.182	7	−1.54	31.166	88.67	0.0	6.4	295	12.4 ± 1.2	66.6 ± 1.0	46.9 ± 1.8	0.70 ± 0.02	0.70	0.26 ± 0.03
284	2007-08-20	488	82.021	86.202	7	−1.55	30.910		0.0	6.9	295	10.6 ± 1.1	65.2 ± 0.7	48.9 ± 1.3	0.75 ± 0.02	0.75	0.22 ± 0.02
285	2007-08-20	726	82.143	86.318	7	−1.62	32.517		5.7	4.8	295	6.3 ± 0.6	68.5 ± 0.8	39.8 ± 1.5	0.58 ± 0.02	0.58	0.16 ± 0.02
285[a]	2007-08-20	726	82.143	86.318	7	−1.62	32.517		5.7	4.8	590	10.5 ± 1.1	67.4 ± 0.6	41.5 ± 1.1	0.61 ± 0.01	0.61	0.25 ± 0.03
290	2007-08-21	2078	82.580	86.423	7	−1.63	33.016	88.31	2.7	0.3	590	11.2 ± 1.1	69.0 ± 0.5	15.1 ± 0.7	0.22 ± 0.01	0.22	0.75 ± 0.08
294	2007-08-22	3148	83.115	86.245	7	−1.67	33.257	83.02			590	11.7 ± 1.2	54.4 ± 0.4	12.6 ± 0.6	0.23 ± 0.01	0.23	0.93 ± 0.10
299	2007-08-23	3693	84.051	89.042	7	−1.69	32.730		5.7	4.0	590	20.9 ± 2.1	65.3 ± 0.6	20.7 ± 0.9	0.32 ± 0.01	0.32	1.01 ± 0.11
301	2007-08-24	3751	84.583	89.820	7	−1.69	32.730				590	21.9 ± 2.2	67.5 ± 0.6	25.3 ± 0.9	0.37 ± 0.01		0.87 ± 0.09
303	2007-08-25	3967	85.243	90.162	7	−1.69	33.602				590	26.3 ± 2.6	65.2 ± 0.7	27.3 ± 1.2	0.42 ± 0.01	0.42	0.96 ± 0.11
309	2007-08-27	4447	87.046	104.714	7	−1.68	31.758	89.26	6.3	10.0	590	25.6 ± 2.6	67.7 ± 0.7	36.0 ± 1.3	0.53 ± 0.02	0.54	0.71 ± 0.08
312	2007-08-29	3046	88.119	120.209	7	−1.65	31.310	88.89	8.5	11.9	590	26.8 ± 2.7	63.0 ± 0.7	39.3 ± 1.3	0.62 ± 0.02	0.64	0.68 ± 0.07
322	2007-08-31	2773	88.127	150.077	7	−1.61	30.635		20.6	11.9	590	32.9 ± 3.3	87.3 ± 0.9	61.5 ± 1.6	0.70 ± 0.02	0.75	0.53 ± 0.06
326	2007-09-01	4022	88.029	170.087	7	−1.51	30.177			14.9	590	43.7 ± 4.4	84.3 ± 0.8	88.9 ± 1.7	1.05 ± 0.02		0.49 ± 0.05
328	2007-09-02	3992	87.833	−170.741	7	−1.55	29.173	90.10	33.1	18.3	590	45.2 ± 4.5	80.0 ± 0.8	85.0 ± 1.8	1.06 ± 0.02	1.19	0.53 ± 0.05
333	2007-09-04	3279	87.028	−146.400	7	−1.53	28.728		49.1	18.0	590	56.2 ± 5.6	87.6 ± 1.4	89.6 ± 2.8	1.02 ± 0.03	1.21	0.63 ± 0.07
335	2007-09-05	2499	86.364	−139.359	7	−1.54	28.475	90.75	75.7	14.8	590	55.2 ± 5.5	90.6 ± 1.1	87.1 ± 2.2	0.96 ± 0.02	1.08	0.63 ± 0.07
338	2007-09-05	1537	85.705	−135.041	7	−1.47	28.585		83.2	11.2	590	58.8 ± 5.9	92.1 ± 1.4	77.4 ± 2.7	0.84 ± 0.03	0.80	0.76 ± 0.08
342	2007-09-07	2302	84.500	−138.419	7	−1.48	29.290		85.1	8.3	590	46.3 ± 4.6	91.7 ± 0.9	57.0 ± 1.5	0.62 ± 0.01		0.81 ± 0.08
346	2007-09-08	2355	84.794	−149.120	7	−1.41	28.242	90.66			585	61.0 ± 6.1	85.8 ± 0.5	91.7 ± 1.1	1.07 ± 0.01		0.67 ± 0.07
349	2007-09-09	2020	85.065	−164.497	7	−1.59	26.911	90.87	70.7	19.0	590	61.6 ± 6.2	94.7 ± 1.5	123.0 ± 3.5	1.30 ± 0.03	1.63	0.50 ± 0.05
352	2007-09-10	4002	86.632	177.590	7	−1.66	29.524				295	47.7 ± 4.8	85.2 ± 1.5	83.7 ± 3.2	0.98 ± 0.03		0.57 ± 0.06
358	2007-09-11	1459	86.506	151.963	7	−1.68	30.892	90.55	9.8	11.9	295	31.8 ± 3.2	70.7 ± 1.1	53.3 ± 2.2	0.75 ± 0.03	0.78	0.60 ± 0.06
363	2007-09-12	3800	86.392	135.847	7	−1.69	31.302		10.7	11.5	295	32.1 ± 3.2	67.7 ± 1.1	51.5 ± 2.1	0.76 ± 0.02	0.79	0.62 ± 0.07
371	2007-09-16	4266	84.661	102.737	7	−1.57	33.157		8.9	9.4	295	38.0 ± 3.8	64.6 ± 0.9	30.5 ± 1.6	0.47 ± 0.02	0.47	1.24 ± 0.14
377	2007-09-18	4347	83.410	115.600	7	−1.65	31.193	89.62			295	35.3 ± 3.5	63.7 ± 0.6	37.4 ± 1.2	0.59 ± 0.01	0.59	0.94 ± 0.10
382	2007-09-19	5345	81.358	120.719	7	−0.97	31.271		0.1	10.6	295	28.6 ± 2.9	62.8 ± 0.9	31.9 ± 1.6	0.51 ± 0.02	0.51	0.90 ± 0.10
385	2007-09-20	3525	79.346	124.347	7	−0.09	31.206		0.0	7.4	285	18.0 ± 1.8	67.6 ± 0.8	31.1 ± 1.4	0.46 ± 0.02	0.46	0.58 ± 0.06
389	2007-09-21	2600	78.355	124.522	7	−1.60	31.466		0.0	7.7	290	19.0 ± 1.9	64.8 ± 0.9	43.8 ± 1.6	0.68 ± 0.02	0.68	0.43 ± 0.05
400	2007-09-22	1041	77.366	123.428	7	−1.60	30.723	89.47	0.0	9.5	295	19.6 ± 2.0	64.8 ± 0.9	49.8 ± 1.7	0.77 ± 0.02	0.77	0.39 ± 0.04
400[b]	2007-09-22	1041	77.366	123.428	7	−1.46	30.723	89.47	0.0	9.5	295	19.1 ± 1.9	67.5 ± 0.9	51.2 ± 1.8	0.76 ± 0.02	0.76	0.37 ± 0.04
400	2007-09-22	1041	77.366	123.428	20	−0.44	33.057	90.59	0.0	5.3	157	14.6 ± 1.5	76.6 ± 1.1	50.9 ± 2.1	0.66 ± 0.02	0.66	0.29 ± 0.03
407	2007-09-23	75	76.181	122.139	7	−1.63	29.531	89.02	0.0		295	16.7 ± 1.7	48.4 ± 0.7	56.2 ± 1.5	1.16 ± 0.03	1.16	0.30 ± 0.03
407	2007-09-23	75	76.181	122.139	65	−1.63	33.812	64.77	0.0	12.7	132	21.7 ± 2.2	95.5 ± 1.2	81.5 ± 2.3	0.85 ± 0.02	0.85	0.27 ± 0.03

Table 4. (continued)

Station	Date	Bottom Depth (m)	Latitude (°N)	Longitude (°E)	Depth (m)	Temperature (°C)	Salinity	Transmission (%)	f_P (%)	f_r (‰)	Volume (L)	^{224}Ra (dpm m^{-3})	^{226}Ra (dpm m^{-3})	^{228}Ra/^{226}Ra	^{228}Ra (dpm m^{-3})	^{228}Ra/^{226}Ra*	^{228}Th/^{228}Ra
407	2007-09-23	75	76.181	122.139	30	−1.58	33.433	86.73	0.0	6.3	129	10.9 ± 1.1	88.6 ± 1.1	0.85 ± 0.02	75.7 ± 2.3	0.85	0.14 ± 0.02
409	2007-09-23	65	75.706	121.770	7	0.78	30.073	89.07	0.0	12.8	295	10.0 ± 1.0	35.4 ± 0.7	1.16 ± 0.04	41.2 ± 1.4	1.16	0.24 ± 0.03
409	2007-09-23	65	75.706	121.770	55	−1.65	33.403	77.36	0.0	9.4	146	6.8 ± 0.7	108.5 ± 2.0	1.08 ± 0.04	117.1 ± 4.5	1.08	0.06 ± 0.01
411	2007-09-24	49	75.201	121.365	7	0.43	29.089	89.32	0.0	13.1	295	9.7 ± 1.0	33.3 ± 0.7	1.02 ± 0.04	34.1 ± 1.5	1.02	0.28 ± 0.03
411	2007-09-24	49	75.201	121.365	40	0.01	32.655	62.43	0.0	14.5	147	13.1 ± 1.3	138.3 ± 1.8	1.75 ± 0.03	242.3 ± 4.9	1.75	0.05 ± 0.01
411	2007-09-24	49	75.201	121.365	25	0.46	32.499	60.90	0.0	15.4	160	47.0 ± 4.7	129.2 ± 1.2	1.91 ± 0.03	247.1 ± 3.2	1.91	0.19 ± 0.02

^{a}Duplicate sample with double sample volume.
^{b}Duplicate sample with loose uncoated acrylic fiber instead of cartridge prefilter.

[*Smith et al.*, 2003; *Kadko and Muench*, 2005; *Lepore et al.*, 2009] are more variable and appear to be strongly affected by biological uptake and release in these productive shelf regions.

[15] Second, offshore surface values in the Eurasian Basin, excluding samples with Pacific influence and samples with significant Ba uptake on the Laptev (Stations 400–411) and Barents (Station 239) shelves (blue symbols without annotation in Figure 2 (top)) have a slight tendency to lower values at higher f_r

$$^{226}\text{Ra} = 71.5 - 56\,f_r;\ R^2 = 0.33,\ n = 26. \qquad (1)$$
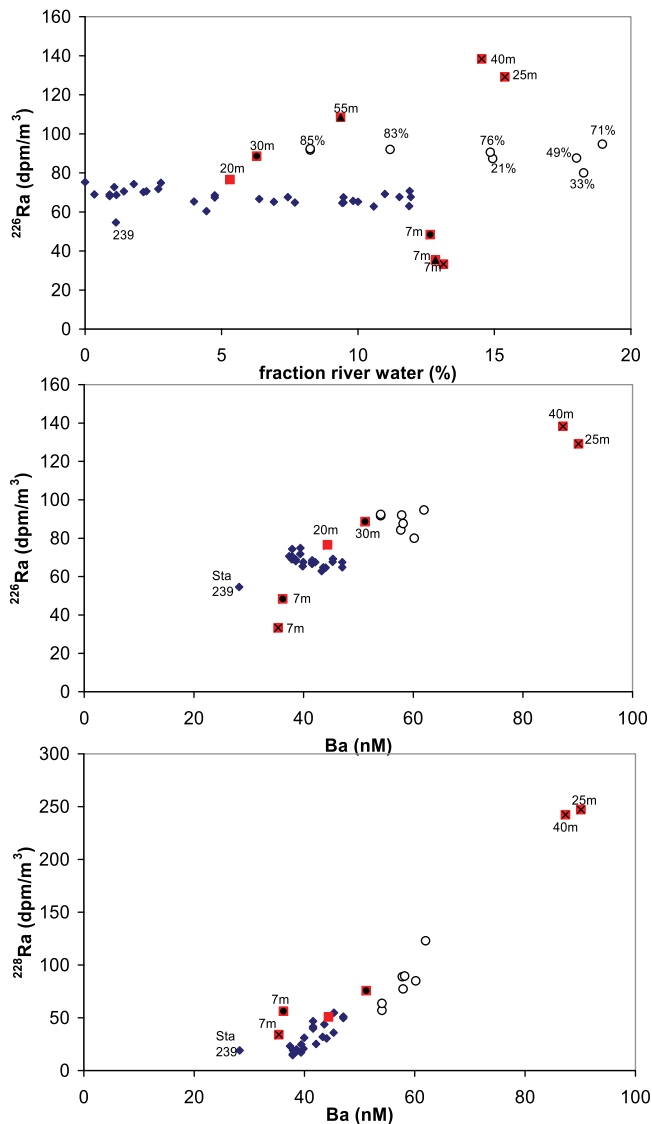
Figure 2. (top) Radium-226 as function of the f_r (fraction of river water), (middle) ^{226}Ra, and (bottom) ^{228}Ra as a function of Ba of all samples shallower than 100 m of ARK XXII/2 (2007) distinguishing samples from the Laptev shelf (red squares with sampling depth and the symbols dot, triangle, and cross identifying stations 407, 409, and 411, respectively) and samples with significant Pacific influence (open circles, as also indicated in Figure 2 (top) by their Pacific water fraction f_P given in %).
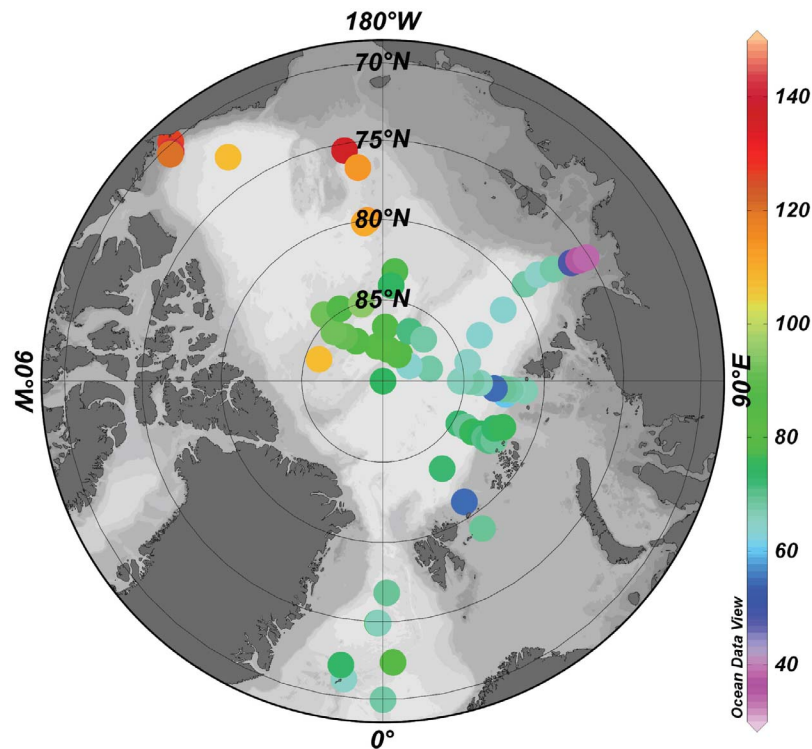
Figure 3. Distribution of [226]Ra (dpm m^{-3}) during ARK XXII/2 compared with literature data (excluding data from the productive Chukchi shelf waters) from GEOSECS Atlantic [*Broecker et al.*, 1976], Cesar Ice Camp [*Moore and Smith*, 1986], TTO [*Key et al.*, 1992], and *Smith et al.* [2003].

[16] This trend can be compared with data from the Kara Sea [*Rutgers van der Loeff et al.*, 2003] that follow the regression [226]Ra = 75.2 − 48 f$_r$;R^2 = 0.91, n = 14, excluding a pure fresh water sample from the Ob river.

[17] And third, on the Laptev shelf, a prominent effect of biological cycling is observed with [226]Ra values in surface waters being reduced by up to 48% relative to equation (1) (Figure 2, top), while they are enhanced in subsurface waters. A reduction is also observed in the surface water at station 239 (cf. Fe data by *Klunder et al.* [2012]). This biological cycling is closely linked to the cycling of Ba [cf. *Guay and Falkner*, 1997; *Abrahamsen et al.*, 2009; *Roeske et al.*, 2012] (Figure 2, middle). Both Ba and [226]Ra are depleted in the Laptev and Barents (Station 239) surface waters, while they show enhanced values in Laptev bottom waters. Moreover, both Ba and [226]Ra show an offset between Eurasian and Pacific surface waters in the central basins [cf. *Roeske et al.*, 2012].

3.2. Radium-228

3.2.1. Distribution of [228]Ra in Summer 2007

[18] The distribution of [228]Ra in 2007 (Figure 4a) shows high values in the TPD. The surface water in the Atlantic inflow and over the Barents shelf has low [228]Ra activities. The maximum activities were found over the Makarov Basin while activities decreased toward the Canadian and Amundsen basins. For comparison with literature observations we also present the [228]Ra data normalized to [226]Ra (Figure 4b). As a result of the Atlantic-Pacific gradient in [226]Ra (Figure 3), the maximum in the [228]Ra/[226]Ra ratio is somewhat shifted toward the Lomonosov Ridge in

comparison with the distribution of [228]Ra, although this is not easily distinguished in the graphs (Figure 4b compared to Figure 4a). Anyhow, the maximum signal in [228]Ra/[226]Ra ratio in the TPD has moved from the Alpha Ridge [*Smith et al.*, 2003] back toward the Lomonosov Ridge (Figure 4b), in agreement with hydrographic observations of this relaxation to anticyclonic, pre-1990s Arctic circulation [*Morison et al.*, 2006]. It should be noted that all samples on the section over the Gakkel Ridge toward the Laptev shelf (section 5) have high [228]Ra activities well in excess of the Atlantic inflow, showing the influence of shelf waters. Surface waters on this section have a substantial river water fraction (about 10%), much larger than further west toward Fram Strait at the longitude of the Voronin Trough (on section 3) where [228]Ra activities were also much lower.

[19] Bottom waters on the shelf are strongly enriched in [226]Ra (Figure 2, middle) but also in [228]Ra (Figure 2, bottom). Even higher enrichment of [228]Ra in bottom waters of the Chukchi shelf has been observed by *Lepore and Moran* [2007]. Diffusive input of the long-lived [226]Ra usually does not cause as prominent an accumulation of [226]Ra in shelf waters as is seen for the shorter-lived [228]Ra. The enrichment of both isotopes in shelf bottom waters therefore implies that the [228]Ra accumulation in bottom waters results not only from a release from shelf sediments but also from biological cycling on the shelf. It is not known whether Submarine Groundwater Discharge contributes to this enrichment.

3.2.2. ARK XI/1: Defining the Freshwater End-Member in the Laptev Sea

[20] Intensive sampling in 1995 (ARK XI/1) provides detailed data to define the [228]Ra source in the Laptev Sea in
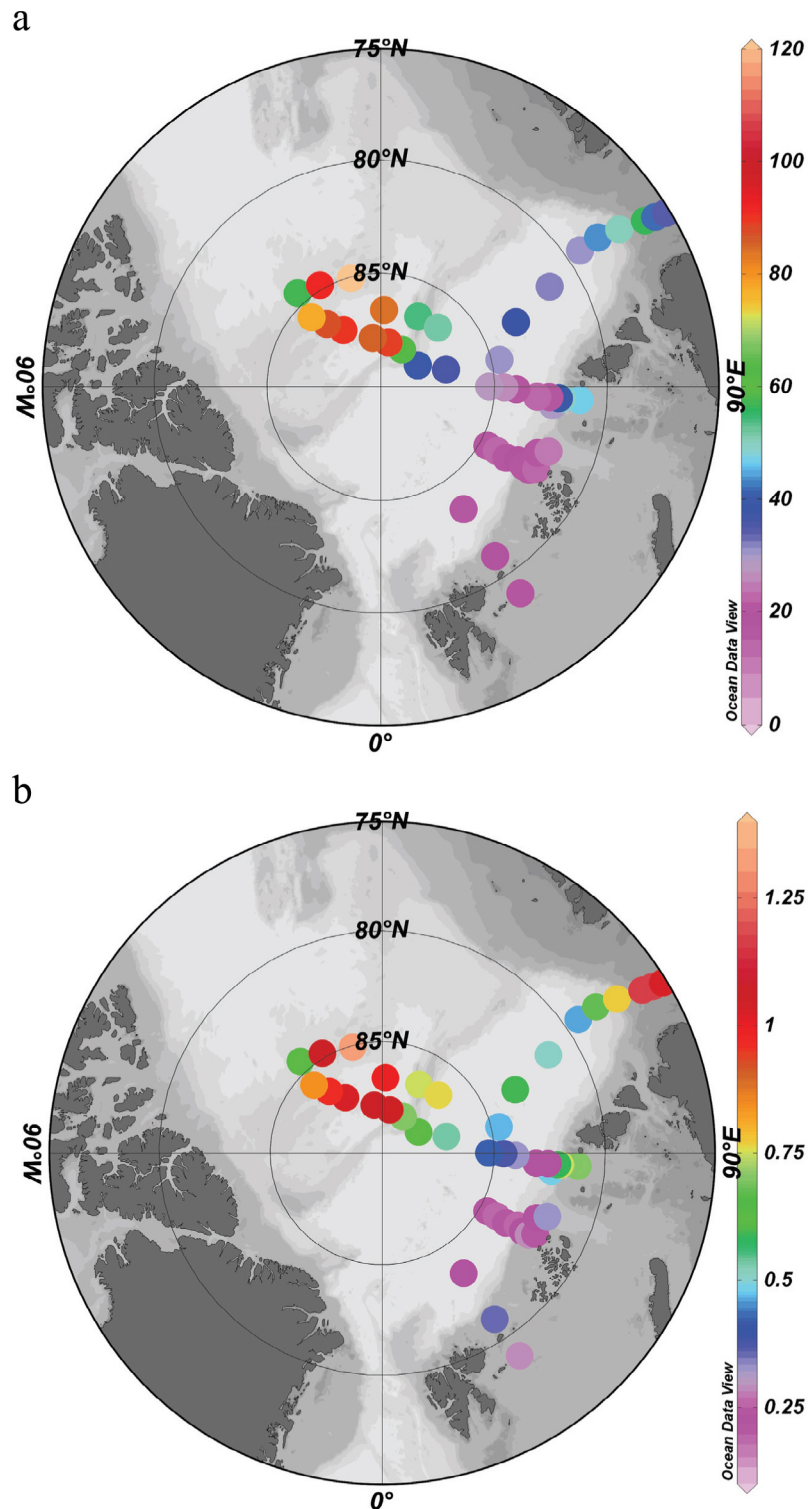
Figure 4. Distribution of (a) ^{228}Ra (dpm m^{-3}) and (b) ^{228}Ra/^{226}Ra ratios in surface waters in summer 2007.

that year. ^{226}Ra and ^{228}Ra activities in the Laptev Sea in 1995 are listed in Table 3. Offshore stations have lower ^{228}Ra activities than most shelf stations when plotted against salinity (Figure 5a). Even if we correct for the dilution by ice meltwater by plotting ^{228}Ra against the fraction of river water using δ^{18}O (Figure 5b), the offshore waters still stand

out by their low ^{228}Ra activities. Essentially the same results are obtained when plotting the ^{228}Ra/^{226}Ra activity ratio (AR) (Figure 5c), implying that the pattern is not a conse- quence of biological uptake/release. This normalization with ^{226}Ra is justified in the Laptev Sea where the fraction of Pacific water can be neglected. The shelf waters correspond
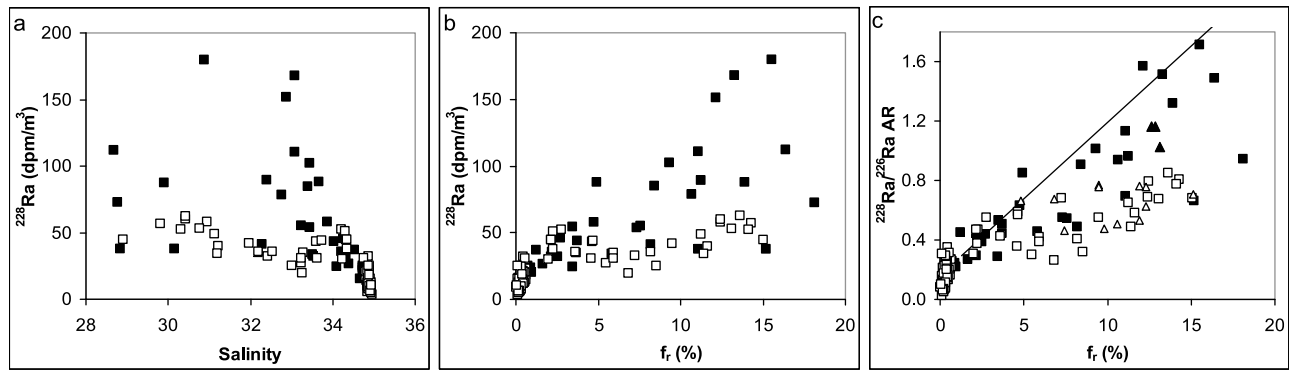
Figure 5. (a) Radium-228 as a function of salinity and (b) as a function of the meteoric fraction f_r and (c) ^{228}Ra/^{226}Ra ratio as a function of the meteoric fraction f_r for all samples of the ARK XI/1 expedition (1995), including samples from the Laptev Sea (<92°N) of the ARK XXII/2 expedition (triangles in Figure 5c), distinguishing shelf (bottom depth < 260 m (closed symbols)) and offshore stations (open symbols) compared in Figure 5c, with the mixing line based on 1991 data from the Eurasian Basin.

well with earlier data from the Laptev shelf [*Rutgers van der Loeff et al.*, 2003]. The low offshore ^{228}Ra activities imply either a freshwater source with lower ^{228}Ra activity from the Kara Sea, or the existence of old recirculated water where ^{228}Ra has decayed.

3.3. Thorium-228/Radium-228

[21] ^{228}Ra decays to ^{228}Th (1.9 years half-life), which in coastal waters is effectively scavenged giving a typical ^{228}Th/^{228}Ra ratio < 0.05 in coastal waters [*Kaufman et al.*, 1981]. Indeed, such low values were also observed in coastal waters of the Canada Basin [*Trimble et al.*, 2004; *Lepore and Moran*, 2007]. Further offshore in the Arctic, we know that Th scavenging rates are very low [*Cai et al.*,

2010], which means that ^{228}Th/^{228}Ra ratios must increase by ingrowth.

[22] The ratio of ^{228}Th to its parent ^{228}Ra (Figure 6) in surface waters over section 3 and section 4 + 5 across the central Arctic Ocean shows how over the deep basins, the absence of strong scavenging allows ^{228}Th to grow into equilibrium with its parent. The ingrowth of ^{228}Th over the deep basins in contrast to the ^{228}Th-depleted shelf waters is clearly seen in a map of ^{228}Th/^{228}Ra in surface water where the present data are compared with literature values (Figure 7). Lowest ratios (<0.3) are observed on the Barents, Kara and Laptev shelf and in the Beaufort Sea. Highest ratios (>0.8) are found in the eastern Eurasian Basin including the section over the Gakkel Ridge and on Ice
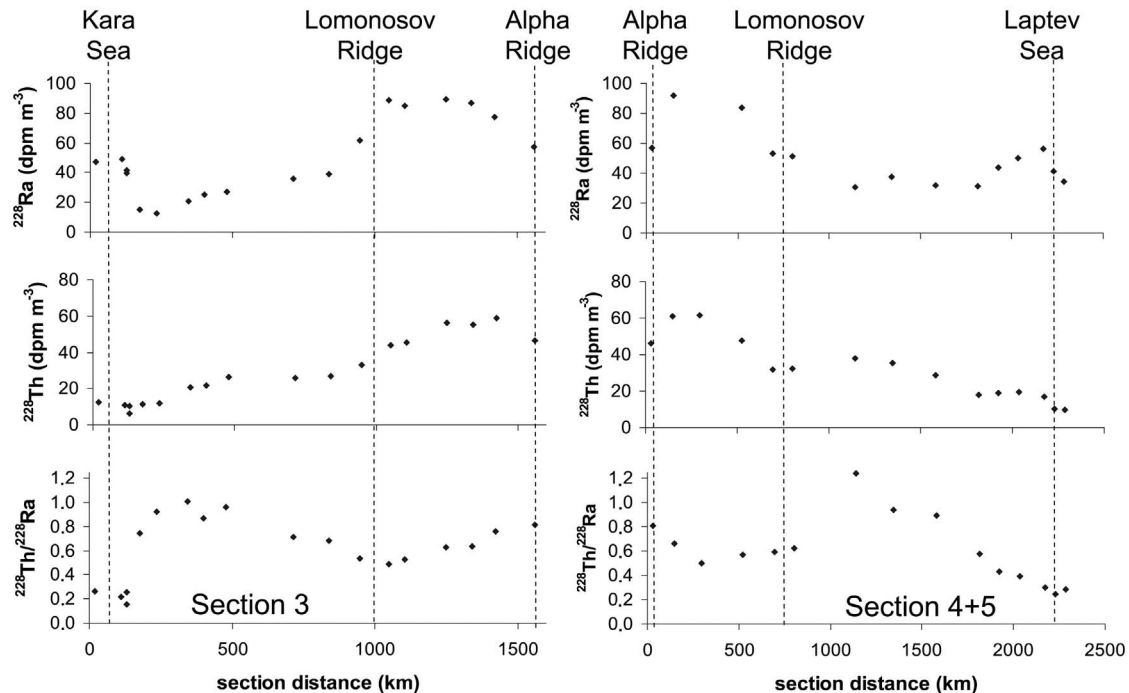
Figure 6. Thorium-228, ^{228}Ra, and ^{228}Th/^{228}Ra ratios in surface water of (left) section 3 (Kara Sea to Alpha Ridge) and (right) section 4 + 5 (Alpha Ridge to Lomonosov Ridge, then over Gakkel Ridge toward Laptev Sea).
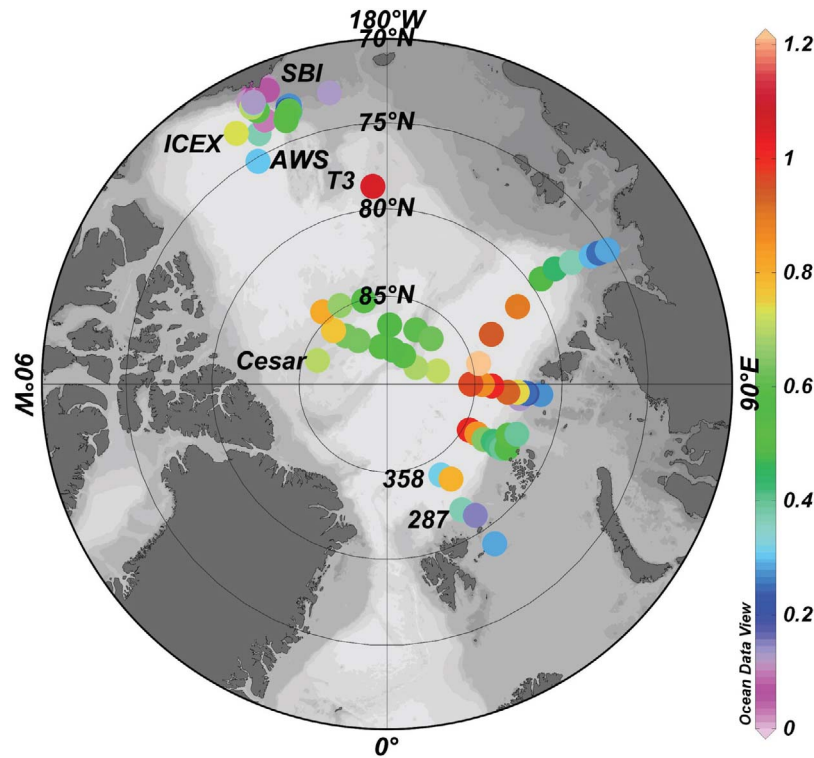
Figure 7. Distribution of ^{228}Th/^{228}Ra ratio in surface waters of ARK XXII/2 (this study) along with literature data (with ranges where symbols overlap) from the Alaskan shelf (Arctic West Summer 2000 (AWS)) [*Trimble et al.*, 2004], ICEX-03 (0.55–0.73) [*Kadko and Muench*, 2005], Chukchi Sea (SBI, spring 0.33 ± 0.27, summer 2002 0.23 ± 0.22, summer 2004, 0.08 ± 0.04 [*Lepore and Moran*, 2007]), Cesar station [*Bacon et al.*, 1989], Ice Island (T3) [*Broecker et al.*, 1973] and the Nansen Basin (stations 287 and 358) [*Cochran et al.*, 1995].

Island T3 in the central Canada Basin. The relatively high AR observed in the low-salinity Polar Surface Layer (PSL) at the ICEX station, only 200 km offshore in the Canada Basin, may be explained if this water represents old recirculated water from the Canada Basin [*Kadko and Muench*, 2005]. These authors also observed high ^{228}Th/^{228}Ra AR on the northern, deep side of their three sections across the Chukchi shelf (their stations 8–18 and 34: depth > 500 m, AR = 0.45 ± 0.08, n = 9). All other stations from that study from the shallower waters in Bering Sea and Chukchi shelf had AR ≤ 0.26 (AR:0.09 ± 0.08, n = 17). The inflow at the Bering Strait has very low ^{228}Th/^{228}Ra AR (<0.06 [*Kadko and Muench*, 2005]). *Lepore and Moran* [2007] showed that the wide variation in ^{228}Th/^{228}Ra ratios on the Chukchi shelf is in part a seasonal phenomenon.

4. Discussion

4.1. Radium-228

4.1.1. Radium-228 Versus ^{228}Ra/^{226}Ra Activity Ratio

[23] As mentioned above, the ^{228}Ra/^{226}Ra AR has often been used instead of the ^{228}Ra activity itself as tracer. This has the advantage of somewhat better analytical precision because usually ^{228}Ra is calculated from a ^{228}Ra/^{226}Ra AR multiplied by the absolute ^{226}Ra activity determined separately. Moreover, the procedure corrects for biological uptake/release. On the Laptev shelf, biological uptake removed 25–48% of ^{226}Ra and 31% of Ba [*Roeske et al.*,

2012] in the surface water (Figure 2). On the other hand, one should always be careful applying a mixing plot using ARs because ratios do not mix linearly [*Kadko and Muench*, 2005] (compare Figure 8). Moreover, in the Arctic we see that there are large differences in ^{226}Ra activity between waters from Atlantic and Pacific origin (Figure 2). In studies like ours with large geographical coverage in the Arctic Ocean, a normalization with ^{226}Ra then requires a correction for the Atlantic/Pacific mixing ratio. For that purpose we introduce here the parameter ^{226}Ra*, in which the ^{226}Ra activity of a sample is corrected for the additional activity it obtained from its Pacific water fraction according to

$$^{226}Ra^* = {}^{226}Ra \frac{(f_P + f_A)^{226}Ra_A}{(f_P {}^{226}Ra_P + f_A {}^{226}Ra_A)}, \qquad (2)$$

where f_A and f_P are the Atlantic and Pacific water fractions and ^{226}Ra$_A$ and ^{226}Ra$_P$ are the ^{226}Ra activities of pure Atlantic and Pacific waters. In equation (2) the numerator $(f_P + f_A)^{226}Ra_A$ gives the ^{226}Ra if all seawater were of Atlantic origin while the denominator $(f_P {}^{226}Ra_P + f_A {}^{226}Ra_A)$ gives the ^{226}Ra expected from a conservative mixing of the two seawater end-members. It should be noted that there are few data for the Pacific source water, and that the ^{226}Ra activity for the northernmost Pacific GEOSECS station 219 (96 dpm/m^3 at 20 m depth) has a Si concentration of 32 μM. If we corrected this for salinity and zero silicate as this was done for Atlantic water by *Cochran et al.* [1995], we would

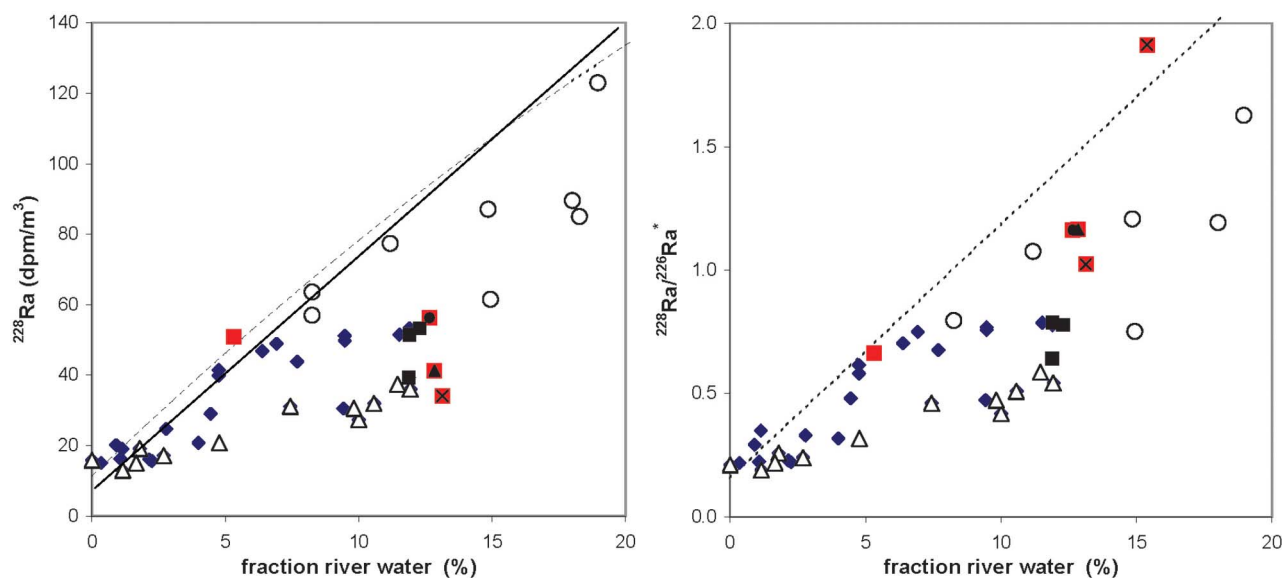**Figure 8.** (left) ^{228}Ra and (right) ^{228}Ra/^{226}Ra* AR as a function of f_r for surface water samples from the ARK XXII/2 expedition (2007) distinguishing samples from the Laptev shelf (red squares, symbols identifying stations 407–411 as in Figure 2), samples with significant Pacific component (open circles) from samples from the Nansen and Amundsen basins (open triangles), close to the Lomonosov Ridge (closed squares, stations 312, 358, 363), and other surface samples (diamonds). The mixing line drawn by eye (straight solid line) is thought to represent mixing of Atlantic inflow with a hypothetical freshwater end-member excluding the samples influenced by biological cycling on the Laptev shelf and is compared here with the ^{228}Ra line (broken line) obtained from the Laptev Sea-Atlantic mixing line of ^{228}Ra/^{226}Ra given by *Rutgers van der Loeff et al.* [1995] multiplied for Figure 8 (left) by ^{226}Ra from equation (1) (Figure 2, top).

find an unlikely ^{226}Ra activity in the Pacific source water of only 44 ± 7 dpm/m^3. The value we use here for ^{226}Ra$_p$, the average of all samples with a Pacific water component > 50% (92.4 ± 1.7 dpm/m^3, n = 4; compare Figure 2 (top)), should therefore not be regarded as the ^{226}Ra of pure Pacific surface water but of the water that has been preconditioned during its passage through the Bering Strait and over the neighboring Arctic shelves. This correction procedure introduces further uncertainties. In the following we therefore prefer to discuss ^{228}Ra activities next to ARs.

4.1.2. Radium-228 as Age Marker

[24] The ^{228}Ra distribution (Figure 4) shows the pathway of the TPD centered over the Makarov Basin with decreasing activities toward the Canada and Amundsen/Nansen basins. This is consistent with maximum concentrations observed for other tracers of terrigenous influences: Fe [*Klunder et al.*, 2012], Mn [*Middag et al.*, 2011], CDOM [*Walker et al.*, 2009; S. A. Walker and R. Amon, personal communication, 2011]. The question we address here is to what extent the deviation from these correlations in the ^{228}Ra data can be interpreted as decay and thus be used as age marker, or rather are due to variability in end-member concentrations. To that effect, we plot the ^{228}Ra activity against the river water component (Figure 8, left). For comparison with literature data where ^{228}Ra has usually been normalized with ^{226}Ra we also show the same data after normalization with ^{226}Ra* in Figure 8 (right).

4.1.3. Formation of ^{228}Ra Excess on the Shelf Produces a Range of End-Members

[25] There are two major sources of ^{228}Ra to the ocean: first, by release from sediments, a source that is particularly important on the vast and shallow Siberian shelves. Some further ^{228}Ra may be released from ice rafted sediments upon ice melt. The second major source is a phase adsorbed to riverine particles that is released in the first stages of estuarine mixing. In the Arctic, the first source is considered much more important than the second [*Rutgers van der Loeff et al.*, 2003, and references therein]. Although this means that the major source of ^{228}Ra in the Arctic does not coincide with the rivers, it has been argued that the combined effect of the river source and the diffuse shelf source on offshore surface waters (i.e., their "far-field" effect) would be similar to the input of a river component carrying a ^{228}Ra signal. A surface water mass in the central Arctic could then be treated as a mixture of ^{228}Ra-poor seawater, ice meltwater and a freshwater component represented by a virtual end-member ^{228}Ra activity. The early data sets in the central Arctic could be well described by this model, although it was questioned whether the various shelf components could be treated as one single end-member composition [*Rutgers van der Loeff et al.*, 1995]. In a subsequent paper we found much lower ^{228}Ra activities at the same salinity or river water fraction in the Kara Sea compared to the Laptev Sea, [*Rutgers van der Loeff et al.*, 2003]. In the Kara Sea the greater depth counteracts the rapid buildup of ^{228}Ra. *Schlosser et al.* [1994] gives an estimate of 3.5 ± 2 years for residence time of fresh water on Siberian shelves. During this time there is an eastward circulation and shallowing depths from the Kara to the Laptev to the East Siberian Sea before the waters turn northward and leave the shelf in the TPD. It is thus likely that ^{228}Ra continues to accumulate eastward and there is no reason why this further accumulation should be correlated
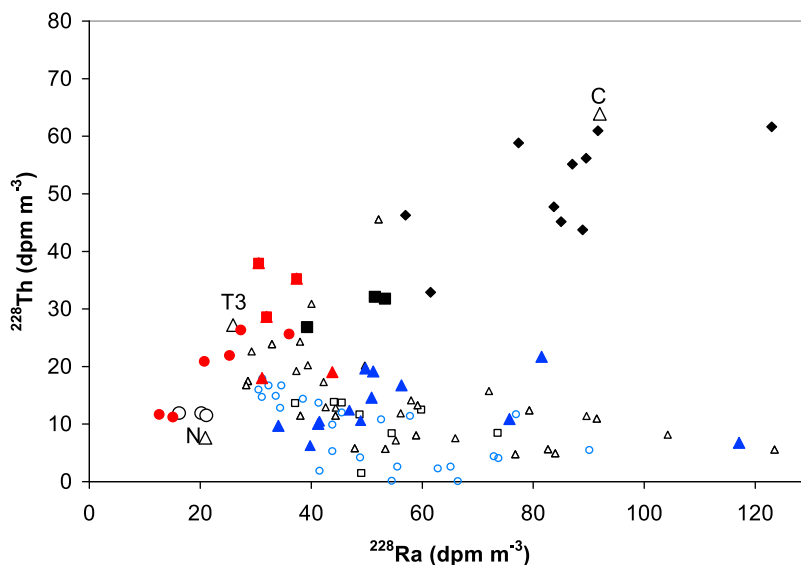
Figure 9. Thorium-228 versus ^{228}Ra in surface waters of ARK XXII/2 (filled symbols distinguishing TPD, black diamonds; Lomonosov Ridge, black squares; Kara and Laptev shelf, blue triangles; Nansen Basin, red circles; north Gakkel Ridge, red squares; southern Gakkel Ridge, red triangles) along with literature data (open symbols) from the Alaskan shelf (AWS, squares) [*Trimble et al.*, 2004], ICEX-03 (large circles) [*Kadko and Muench*, 2005], Chukchi Sea (SBI, small circles [*Kadko and Muench*, 2005], triangles [*Lepore and Moran*, 2007]), Cesar station (C) [*Bacon et al.*, 1989], Ice Island (T3) [*Broecker et al.*, 1973] and the Nansen Basin station studied by Cochran (N) [*Cochran et al.*, 1995].

with continued freshwater inputs. This is why we concluded that water may thus reach the shelf edge with variable shelf signatures [*Rutgers van der Loeff et al.*, 2003].

[26] The low ^{228}Ra activities observed offshore in the Laptev Sea during 1995 (Figure 5) could indeed be interpreted to result from a low-^{228}Ra freshwater source, e.g., from the Barents or Kara Sea. This distribution is confirmed by the data of the 2007 expedition. Surface samples (with $f_r > 2.5\%$) from the Laptev shelf of both expeditions have high ^{228}Ra activities in agreement with the mixing line based on 1991 data from the Eurasian Basin [*Rutgers van der Loeff et al.*, 1995]. Surface samples of stations with > 260 m bottom depth of both expeditions have ^{228}Ra activities that are only about half those predicted by the conservative, nondecayed mixing line (Figure 5c).

[27] At this point it cannot be decided whether the low offshore ^{228}Ra activities are due to a lower freshwater end-member activity advected from the Kara Sea, or result from decay which would imply that the offshore surface waters contain a river water fraction with a long residence time in the deep Eurasian Basin.

[28] This situation is very similar to the distribution observed by *Kadko and Muench* [2005] in the Beaufort Sea. These authors observed much lower ^{228}Ra activities in offshore low-salinity Polar Surface Water (Polar Surface Layer, PSL) and concluded that these were waters that had been recirculating in the Canada Basin. They used the ^{228}Ra activities to estimate the age of the PSL water to be up to 14 years. But also in the Canada Basin the actual freshwater ^{228}Ra end-member is not well constrained, and a rigorous distinction between variability in source concentration and radioactive decay cannot be made. In the following we will use the additional tracer ^{228}Th/^{228}Ra to distinguish between these alternative explanations.

4.2. Thorium-228/^{228}Ra Ratios

[29] Here we will investigate to what extent the ingrowth of ^{228}Th into the shelf-induced ^{228}Ra can itself serve as a time marker. For this discussion it is essential to know the isotope composition of the water that constitutes the source of the Ra in the central Arctic ocean. In Figure 7 we have seen the gradual increase of ^{228}Th/^{228}Ra AR from shelf to central ocean, but the differences are even more apparent in a plot of ^{228}Th versus ^{228}Ra (Figure 9). There is a large variation in concentrations on the shelves and part of the variation in ^{228}Th/^{228}Ra AR is seasonal [*Lepore and Moran*, 2007]. While plankton growth and export leads to the removal of thorium, there is also a significant uptake of radium (Figure 2), which might even contribute to the sometimes relatively high AR values in shelf waters with low ^{228}Ra (Figure 9). However, these ^{228}Ra-depleted shelf waters clearly cannot be the source of the high ^{228}Ra activities in the TPD (51–92 dpm m^{-3} and one exceptionally high value of 123 dpm m^{-3}, Station 349). Instead we must look for source waters with at least a similarly high ^{228}Ra activity. At high ^{228}Ra activities (>80 dpm m^{-3}) the ^{228}Th/^{228}Ra AR is only 0.1–0.2 (Figure 9) and in the following we will assume that the ^{228}Ra-enriched shelf water leaves the shelf with an AR $F_0 = 0.15 \pm 0.05$. As we will show later, the age estimates are not very sensitive to errors in F_0.

4.3. Models for the Distribution of ^{228}Ra and ^{228}Th

4.3.1. Constant ^{228}Ra: Concordia With ^{234}Th/^{238}U

[30] In a system with a constant ^{228}Ra (and ^{238}U) activity and a constant scavenging rate of Th, the steady state ^{228}Th/^{228}Ra values should be concordant with ^{234}Th/^{238}U ratios [*Kaufman et al.*, 1981]. Indeed, the range of values we observed on the shelf is concordant with observed
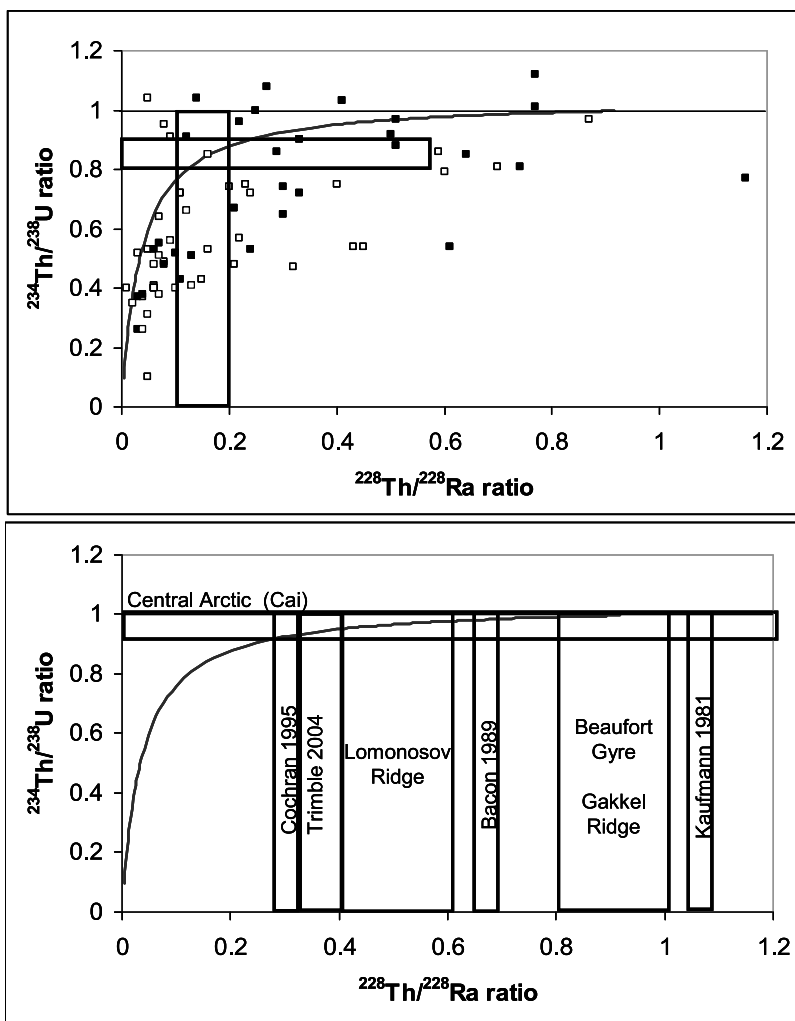
Figure 10. Observed range of ^{234}Th/^{238}U versus ^{228}Th/^{228}Ra compared with the theoretical steady state "concordia" line [*Kaufman et al.*, 1981; *Lepore and Moran*, 2007] in (top) shelf stations of Laptev Sea (boxes, this study, and *Cai et al.* [2010]) and Chukchi Sea (distinguishing summer (open symbols) and spring (closed symbols) [*Lepore and Moran*, 2007]) and (bottom) central Arctic for this study (Lomonosov Ridge, ^{228}Th/^{228}Ra AR 0.4–0.6; Beaufort Gyre and Gakkel Ridge AR 0.8–1.0) compared with literature AR values of *Cochran et al.* [1995], *Trimble et al.* [2004] (AWS 3: 0.30 ± 0.03 AWS 4: 0.37 ± 0.06), *Bacon et al.* [1989], and *Kaufman et al.* [1981].

^{234}Th/^{238}U ratios of 0.8–0.9 [*Cai et al.*, 2010] (Figure 10, top).

[31] A similar calculation can be made for the deep basins. Here, the very low thorium scavenging rates found by *Cai et al.* [2010] must allow ^{228}Th activities to increase. Outside the more productive shelf regions the depletion of ^{234}Th with respect to ^{238}U was largely limited to the upper mixed layer which was usually only approx 20 m deep. In 30 stations over the slope and the central basin ^{234}Th/^{238}U in the surface layer (5 m depth) was 0.89 ± 0.11. But the depletion follows a distinct geographical trend ((Figure 11) data from *Cai et al.* [2010]). The five stations on the Barents slope (depth range 1533–3115 m) stand out by strong depletion (^{234}Th/^{238}U < 0.8) (Figure 11, right), which we attribute to export related with production influenced by the Barents shelf [*Wassmann et al.*, 1999, 2004; *Lalande et al.*, 2008], as was also observed in Ba [*Roeske et al.*, 2012] and Fe

[*Klunder et al.*, 2012] data. Excluding the Barents slope, the average ^{234}Th/^{238}U in the surface layer of all stations with depth > 1500 m was 0.942 ± 0.060 (n = 18) in good agreement with the data from three permanently ice-covered stations in the Canada Basin sampled by *Trimble and Baskaran* [2005] (0.946 ± 0.057). If we restrict the region further to the central Arctic N of 84°35′N the average becomes 0.958 ± 0.058 (n = 11). These ^{234}Th/^{238}U ratios correspond in steady state to a thorium scavenging rate of 0.46 (0–1.16) y^{-1}. Again in steady state, this would cause a ^{228}Th/^{228}Ra ratio of 0.24–1.0. Indeed, in the central Eurasian and Canada basins ^{228}Th/^{228}Ra ratios (our own and literature values) are far above the ratio of shelf waters (Figures 6, 7, and 9). But apart from the crude comparison in Figure 10, the concordia concept is not a satisfactory description of the data. The isotope distribution cannot be described as steady state because, as we shall see, ingrowth of ^{228}Th causes
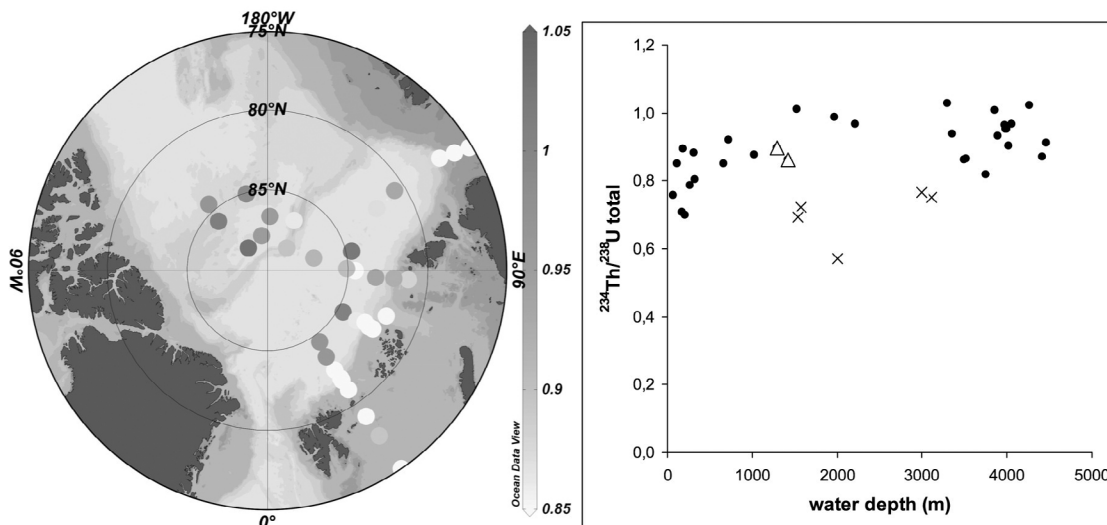
Figure 11. ^{234}Th/^{238}U ratio in surface waters as a function of (left) geographical location and (right) bottom depth, distinguishing stations over Lomonosov Ridge (open triangles) and Barents shelf (crosses) from other stations (dots). Data of *Cai et al.* [2010].

gradual changes in the ^{228}Th/^{228}Ra ratio. Seasonal variations are a further cause of large deviations from concordia, especially in shelf areas [*Lepore and Moran*, 2007].

4.3.2. Open System Approach: Eddy Diffusion

[32] In ocean margins where ^{228}Ra is released from coastal sediments and where coastal waters exchange with offshore waters by horizontal mixing (eddy diffusion), ^{228}Ra decreases exponentially with distance offshore by horizontal mixing and decay. In these systems the distribution of ^{228}Th (activity A_T) is governed by decay of ^{228}Ra (activity A_R), ingrowth and scavenging of ^{228}Th (scavenging rate λ_s) and mixing, as discussed by *Broecker et al.* [1973]:

$$\lambda_R A_R = k\frac{\partial^2 A_R}{\partial x^2} \tag{3}$$

$$(\lambda_T + \lambda_s)A_T = A_R\lambda_T + k\frac{\partial^2 A_T}{\partial x^2}, \tag{4}$$

where k is the horizontal eddy diffusion coefficient, x is distance offshore and λ_R and λ_T are the decay constants of ^{228}Ra and ^{228}Th, respectively. The offshore distribution of ^{228}Ra follows a simple exponential decay [*Broecker et al.*, 1973]:

$$A_R = A_{R^0}e^{-\sqrt{\frac{\lambda_R}{k}}x}, \tag{5}$$

where the superscript ° denotes the situation when the water leaves the shelf. For the boundary condition of a constant ^{228}Th/^{228}Ra AR on the shelf (F_0) we find the solution:

$$A_T = \frac{\lambda_T A_{R^0}}{\lambda_T + \lambda_s - \lambda_R}e^{-\sqrt{\frac{\lambda_R}{k}}x} + (F_0 A_{R^0} - \frac{\lambda_T A_{R^0}}{\lambda_T + \lambda_s - \lambda_R})e^{-\sqrt{\frac{\lambda_T + \lambda_s}{k}}x}, \tag{6}$$

which for the condition of 100% scavenging on the shelf ($F_0 = 0$) simplifies to [*Broecker et al.*, 1973]

$$A_T = \frac{\lambda_T A_{R^0}}{\lambda_T + \lambda_s - \lambda_R}(e^{-\sqrt{\frac{\lambda_R}{k}}x} - e^{-\sqrt{\frac{\lambda_T + \lambda_s}{k}}x}) \tag{7}$$

[33] Equations (5) and (6) define a relationship between ^{228}Th and ^{228}Ra,

$$A_T = \frac{\lambda_T}{\lambda_T + \lambda_s - \lambda_R}A_R + (F_0 - \frac{\lambda_T}{\lambda_T + \lambda_s - \lambda_R})A_{R^0}\left(\frac{A_R}{A_{R^0}}\right)^{\sqrt{\frac{\lambda_T + \lambda_s}{\lambda_R}}}, \tag{8}$$

which is displayed in Figure 12 for several values of the Th scavenging rate and a shelf source with a ^{228}Th/^{228}Ra AR $F_0 = 0.15$. We have already seen that the ^{228}Ra activity of this source is not well constrained. Based on the distribution of concentrations in shelf waters we use here 110 dpm m^{-3} although locally activities up to 180 dpm m^{-3} are found (Table 3), and even higher in bottom waters on the shelves. With these assumptions, the mixing model cannot explain our data. This conclusion is not affected by possible changes in F_0 (broken lines in Figure 12) as might, e.g., result from our overestimate of ^{228}Th on the shelf due to excess ^{224}Ra. Especially for the high ^{228}Ra activities we observed in the TPD, the high-^{228}Th data are incompatible with the mixing model, even in the absence of scavenging ($\lambda_s = 0$). The continued exchange in this model with the Th-depleted shelf water does not allow Th to grow to the high values observed offshore.

4.3.3. Closed System Approach: Advection

[34] Neither the steady state model with constant ^{228}Ra and ^{238}U activities leading to a concordia with ^{234}Th/^{238}U, nor a mixing model based on eddy diffusion gives an appropriate representation of the situation in the central Arctic. Here the surface circulation is characterized by the TPD. When the shelf waters turn offshore, lose contact with
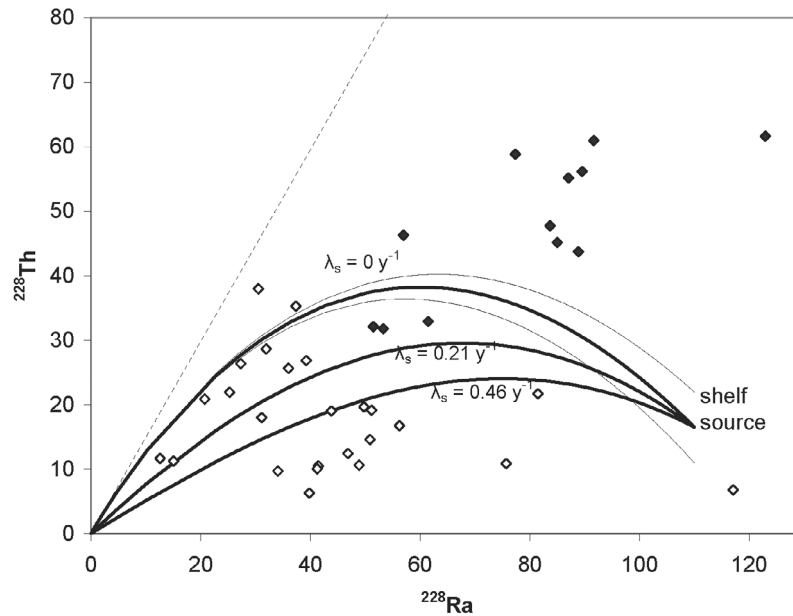
Figure 12. Thorium-228 versus ^{228}Ra (dpm m^{-3}) in surface waters of this study (TPD, filled symbols) compared with horizontal mixing model for $\lambda_s = 0$ (including results for $F_0 = 0.1$ and 0.2, thin lines), 0.21 and 0.46 y^{-1}. In the case without scavenging ($\lambda_s = 0$), the results approach at high distance offshore the limiting AR of $\lambda_T /(\lambda_T - \lambda_R) = 1.49$ (straight broken line).

the shelf and flow as a thin lens over deep water, ^{228}Ra is no longer supplied by the sediments and will decay. At the same time, the reduction in scavenging rate will allow the gradual ingrowth of ^{228}Th. In this advective system it is more appropriate to calculate the time development of parent and daughter as the net result of decay of ^{228}Ra, ingrowth of ^{228}Th and removal of ^{228}Th by scavenging, but without

horizontal mixing. If we assume that the scavenging is reduced to a low open ocean value as soon as the water mass leaves contact with the shelf, the ingrowth of ^{228}Th will follow the two-decay curve:

$$A_T = A_{T^0} e^{-(\lambda_T + \lambda_s)t} + \frac{\lambda_T + \lambda_s}{\lambda_T + \lambda_s - \lambda_R} A_{R^0} \left(e^{-\lambda_R t} - e^{-(\lambda_T + \lambda_s)t} \right), \quad (9)$$
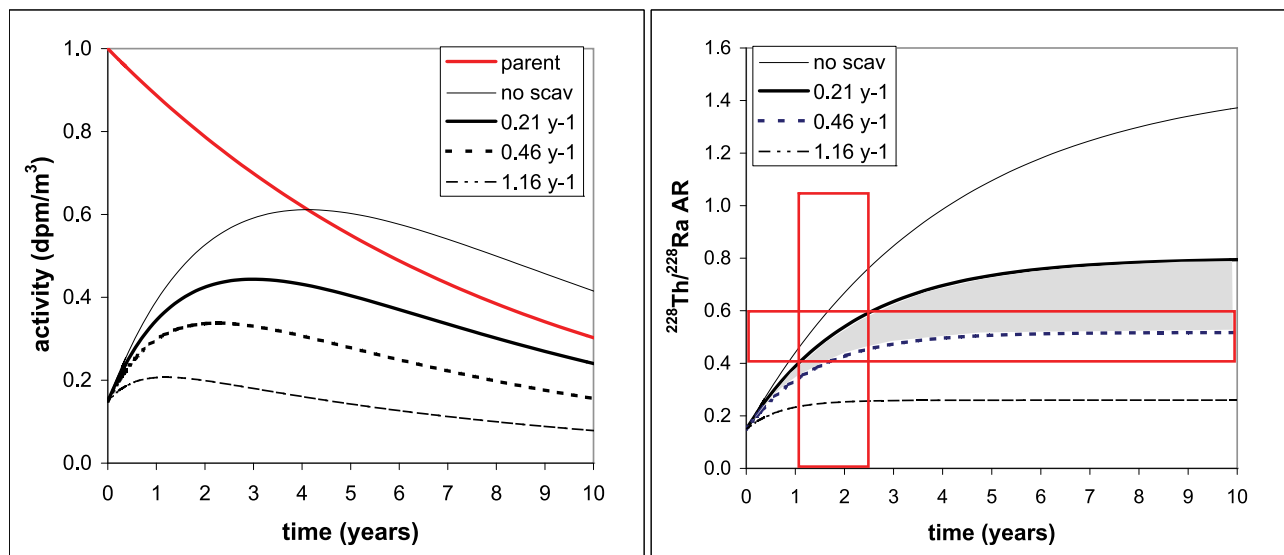
Figure 13. Evolution of (left) ^{228}Ra (parent, with arbitrary initial activity) and ^{228}Th activity and (right) ^{228}Th/^{228}Ra ratios for several values of the scavenging constant λ_s as function of time after contact with the shelf source. The range compatible with measured ^{234}Th/^{238}U ratios is shaded. At a (^{234}Th-based) scavenging rate of 0.46 y^{-1}, an AR of 0.4 is reached after 1.6 years while an AR of 0.6 is incompatible with this scavenging rate. Using $\lambda_s = 0.21$ y^{-1}, the AR of 0.4–0.6 is reached 1–2.5 years after leaving the high-scavenging shelf regime (highlighted by boxes).
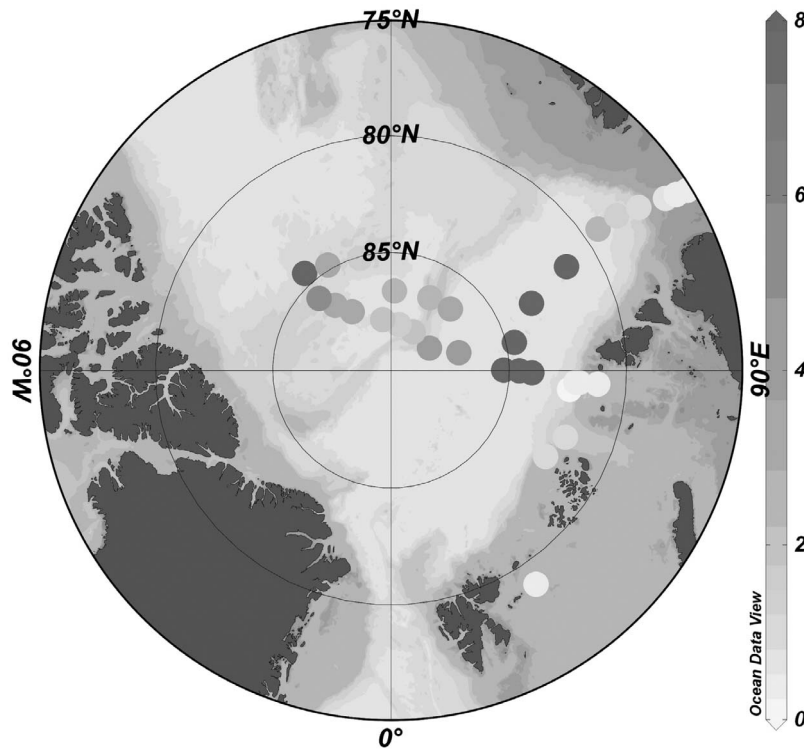
Figure 14. Age (years) of shelf waters based on equation (9) and assuming a constant Th scavenging rate λ_s of 0.21 y^{-1}, omitting the stations in the Atlantic inflow identified by ^{228}Ra < 20 dpm/m^3. Darkest circles have a model age > 8 years.

where the superscript ° again denotes the situation a t = 0 when the water leaves the shelf. This model does not include mixing. There is a strong vertical gradient in ^{228}Ra activity in the halocline [*Rutgers van der Loeff et al.*, 1995]. Although stratification is strong, mixing will cause some loss of ^{228}Ra to deeper waters. As the ^{228}Th gradient is in the same direction, the ratio should not be strongly affected by this loss by mixing.

[35] In Figure 13 the evolution of ^{228}Th and of the ^{228}Th/^{228}Ra AR has been modeled for several values of λ_s. Note that the evolution of the AR in this model is independent on the actual value of ^{228}Ra in the shelf source. An error in the value used for F$_0$ causes a relatively small error in the predicted ages. If for example a water parcel leaves the shelf with an F$_0$ of 0.1, it would take just 2–3 months for the ingrowth to reach the value of 0.15, the starting point of our model calculations.

[36] The model results show that many observed ^{228}Th/^{228}Ra ratios in the central Arctic Ocean (Figure 7) can never be reached with the ^{234}Th-based average scavenging rate of 0.46 y^{-1}. The observed ^{228}Th/^{228}Ra ratio of 0.8 sets an upper limit to λ_s of 0.21 y^{-1}. This can be explained when the scavenging rate over the longer time horizon recorded by ^{228}Th is lower than the recent summer value recorded by the short-lived ^{234}Th. Based on the ingrowth model, we can now derive an age since the water mass detached from the shelf area. In a first approximation, we assume that $\lambda_s = 0.21$ y^{-1} throughout the deep Arctic Ocean and determine the age based on the ^{228}Th/^{228}Ra ingrowth using equation (9). The results (Figure 14) confirm the high age of the fresh water component observed in the central Eurasian Basin over the

Gakkel Ridge. Even in the absence of scavenging, ingrowth to the AR values observed at stations 371–382 (0.90 ± 0.10 to 1.24 ± 0.13) requires 2.7–4.1 to > 5.2 years, respectively. This is a strong argument that the low ^{228}Ra values observed offshore in the Laptev Sea in 1995 and 2007 (Figure 5c) are due to decay during recirculation of these waters and not to an input of low-radium water from the Kara Sea.

[37] In the age calculation above we have assumed that once the water has left the shelves, the scavenging rate is everywhere the same. The high-^{228}Th/^{228}Ra ratios in the Nansen Basin of 0.8 require an ingrowth period of at least 3 years even if no scavenging had occurred. But the reduced ^{228}Th/^{228}Ra ratios over the Lomonosov Ridge and over the southern part of the Gakkel Ridge could be explained either by a rapid transport from the shelf or by a somewhat higher-scavenging rate. We have therefore looked for indications of spatial differences in suspended particulate material and scavenging rates.

4.4. Evidence for Regional Differences in Scavenging Rates

4.4.1. Transmissometry

[38] The clearest waters, as deduced from transmissometer readings (Figure 15) were found over the Nansen Basin and in the Makarov/Alpha Ridge region. Light transmission was reduced over the Amundsen Basin and Lomonosov Ridge and over most of section 5 over the Gakkel Ridge toward the Laptev shelf.

4.4.2. Particulate ^{234}Th

[39] Particulate ^{234}Th in surface water can be considered as a proxy for the suspended matter load [*Rutgers van der*
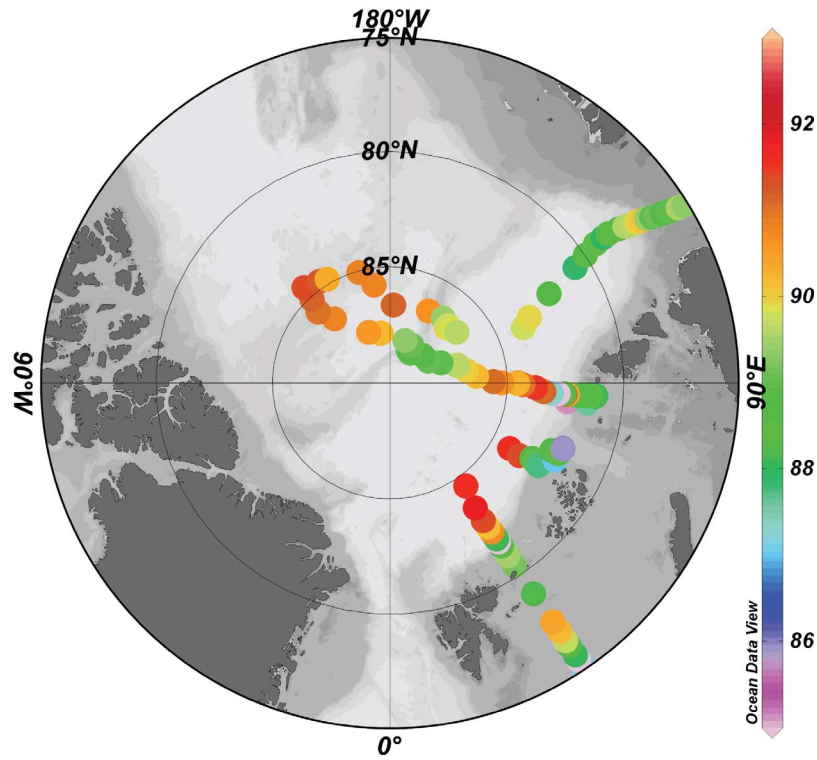
Figure 15. Light transmission (%) at 10 m depth during expedition ARK XXII/2.

Loeff et al., 2011]. Indeed, the distribution of particulate ^{234}Th (Figure 16) resembles well the distribution of light transmission, with the same features: relatively high values during passing of the Lomonosov Ridge, especially during

the first section (3). On the second section (4) we observed again enhanced values, then especially on the Amundsen side of the Lomonosov Ridge. We found enhanced values also over most of section 5 over the Gakkel Ridge toward
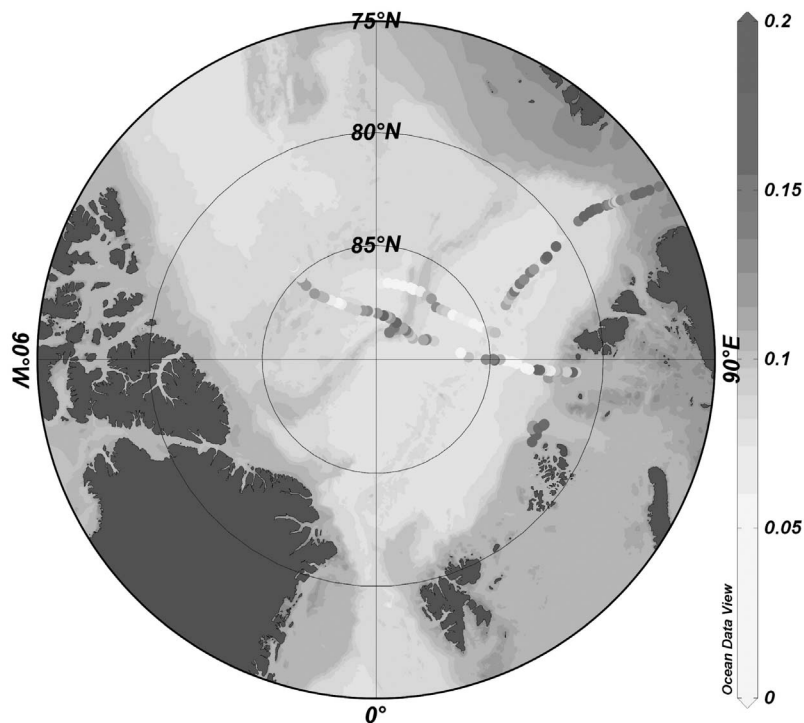
Figure 16. Particulate ^{234}Th/^{238}U as monitored with the automatic ^{234}Th sampler.

the Laptev Sea and slightly enhanced values over the Alpha Ridge. The lowest values, corresponding to the clearest water, were found in the Nansen Basin, the Siberian side of the Amundsen Basin and the southern part of the Makarov Basin. The large differences between the two sections over the Makarov Basin point at temporal changes in the composition of the TPD. *Bauch et al.* [2011] came to a similar conclusion based on δ^{18}O data from these sections.

4.4.3. Total ^{234}Th/^{238}U: Export From Surface Layer

[40] In the far offshore region with latitude > 84°35′ we had found from the data of *Cai et al.* [2010] an average ^{234}Th/^{238}U ratio of 0.958 ± 0.058 (n = 11). The nine stations with depth > 1500 m (depth > 1500 m, lat > 84°35′) have ^{234}Th/^{238}U = 0.975 ± 0.047 (n = 9). The two stations close the Lomonosov Ridge stand out with ^{234}Th/^{238}U values of 0.90 ± 0.04 (Sta 316, 1298 m bottom depth) and 0.86 ± 0.04 (Sta 358, 1424 m). The ^{234}Th/^{238}U ratio of 0.90 observed over the Lomonosov Ridge (station 316, 30 August: 0.90 ± 0.04; station 358, 11 September: 0.86 ± 0.04.) corresponds in steady state with a scavenging rate of 1.17 y^{-1}.

[41] With this scavenging rate, the ^{228}Th/^{228}Ra AR could not have increased above 0.26 (Figure 13, right). As we observed a ratio of 0.5, we again conclude that the scavenging must have been seasonally increased. The Th scavenging rate observed from ^{234}Th/^{238}U disequilibrium in summer 2007 may thus represent a maximum over a year as primary productivity is typical at its highest in this season. Also, particle export studies using sediment traps indicate that POC export is at its highest in summer [*Cai et al.*, 2010, and references therein]. Therefore, there is a good reason to use for λ_s a lower year-round average value than the one calculated using summer ^{234}Th data. A short summer increase in λ_s would also affect ^{228}Th activities, but the relative effect would be smaller for the longer lived ^{228}Th, which would already be depleted by about 50% before the summer, than for the short-lived ^{234}Th, with a depletion of only 10%.

[42] The combined evidence (Figure 17) infers an enhanced particle load and scavenging rate in the area of the Lomonosov Ridge. Apparently, the shelf input in this region is so large that even this far offshore it enhances productivity and export above the neighboring regions. It is also likely that the increased particle load and scavenging rate is related to the release of ice-rafted particles upon ice melt [*Baskaran et al.*, 2003; *Trimble and Baskaran*, 2005].

4.5. Synthesis/Comparison of the Models

[43] In Figure 18 we compare our and selected literature data of ^{228}Th and ^{228}Ra in surface waters of the offshore Arctic Ocean with the predictions of the various models discussed. All stations are sufficiently far offshore that excess ^{224}Ra must have decayed and the measured ^{224}Ra is a good proxy for ^{228}Th. The observations in the TPD, especially all samples with ^{228}Ra > 75 dpm m^{-3} (stations 322–352 or all stations on the Canadian side of the Lomonosov Ridge, Cesar station) are incompatible with the mixing model at any value of λ_s and best explained by the advective model. The values over the Lomonosov Ridge are also incompatible with the mixing model if we realize that scavenging cannot be disregarded here. Based on the ^{228}Th/^{228}Ra ingrowth in the advective model (Figure 13), the minimum shelf water age of surface waters (disregarding

scavenging) in the TPD ranges from 1.2 years near the Lomonosov Ridge (AR = 0.49) to 2.7 years in the Makarov Basin/Alpha Ridge (AR = 0.79). With the evidence of enhanced scavenging rates over the Lomonosov Ridge it is more likely that the age of water over that Ridge is rather ≥3 yr.

[44] The interpretation of the data in the Eurasian Basin is more difficult because the ^{228}Ra activities are much lower and for these activities the model results tend to approach each other. Nevertheless, the high AR for the samples over the northern part of the Gakkel Ridge require time to accumulate. In the advective model, the AR of 0.9 and above would not be reached before 3.4 years, even disregarding scavenging. The ^{228}Th accumulation over the Gakkel Ridge shows that the surface water cannot flow here in parallel to the TPD with the rate experienced for the ice by the Tara drift. It is more likely that a recirculating gyre exists, increasing the residence time of the surface water in the Eurasian Basin.

5. Conclusions

[45] Similar to Ba, Ra is clearly affected by biological uptake in surface waters of the Arctic shelves and release in their bottom waters. The biological effect on ^{228}Ra distribution can be corrected for by normalizing with ^{226}Ra. But ^{226}Ra also resembles Ba in enhanced concentrations in waters of Pacific origin compared to waters of Atlantic origin. This difference has to be accounted for when ^{228}Ra/^{226}Ra ratios are used in pan Arctic studies.

[46] In the central Arctic, ^{228}Ra is at its maximum over the Lomonosov Ridge and Makarov Basin. If the maximum has moved toward the Canada Basin in the early nineties [*Smith et al.*, 2003], it has moved back with the change to more anticyclonic surface water circulation [*Morison et al.*, 2006].

[47] The half-life of ^{228}Ra (5.8 years) is appropriate for the study of shelf water transport in the TPD. But the use of ^{228}Ra as age marker for shelf waters requires that the shelf source of ^{228}Ra is constant in space and time. Judged from the transit times of ice (1.5–4 years) and surface water (minimum estimate 2–5 years [*Schlosser et al.*, 1999]) the initial ^{228}Ra must be known to clearly better than 50%. We cannot judge whether this condition is met to a sufficient extent to allow the calculation of ages with acceptable error limits for the relatively rapid transport in the TPD.

[48] Seasonal removal of Th and Ra produces a wide range of ^{228}Ra activities and ^{228}Th/^{228}Ra ratios on the shelves. The high ^{228}Ra activities in the central Arctic Ocean imply that these Ra-depleted shelf waters cannot be the source for the TPD. Shelf waters with sufficiently high ^{228}Ra activity (>100 dpm m^{-3}) usually have low ^{228}Th/^{228}Ra (AR < 0.2), and we assume that these waters leave the shelf with a ^{228}Th/^{228}Ra activity ratio (F_0) of 0.15 ± 0.10. ^{228}Th/^{228}Ra ratios in surface waters increase through 0.4–0.6 in the TPD over the Lomonosov Ridge to 0.8–1.0 over the deep basins. The ingrowth of ^{228}Th into its ^{228}Ra parent thus provides independent age information of surface waters. However, the interpretation of this information with an ingrowth-scavenging model is complicated by clear geographical differences in scavenging rates. Transmission, particulate ^{234}Th, and ^{234}Th/^{238}U data consistently show

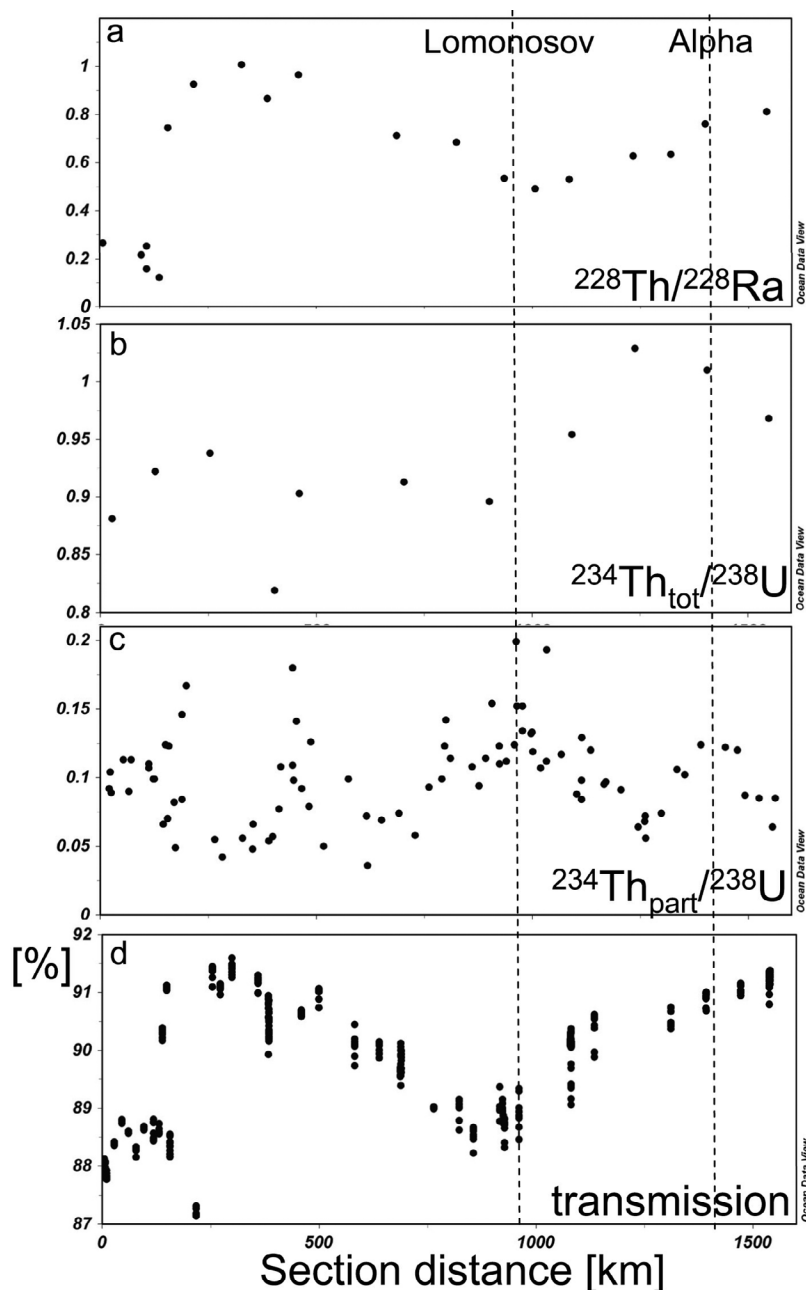**Figure 17.** (a) ^{228}Th/^{228}Ra ratio compared with (b) total ^{234}Th/^{238}U ratio [*Cai et al.*, 2010], (c) particulate ^{234}Th/^{238}U ratio (automatic filtration), and (d) beam transmission (CTD casts) in surface water of section 3, showing enhanced suspended load and scavenging near Lomonosov Ridge.

enhanced suspended particulate matter concentrations and correspondingly high-scavenging rates over the Lomonosov Ridge compared to the adjacent deep basins.

[49] The minimum shelf water age of surface water over the Lomonosov Ridge, estimated with neglect of scavenging, is 1.1 yr. With the evidence of enhanced scavenging rates over the Lomonosov Ridge it is more likely that the age of water over that Ridge is rather ≥3 yr. The surface water on the Canadian side of the TPD is older as has been shown in previous studies [*Rutgers van der Loeff et al.*, 1995; *Hansell et al.*, 2004; *Letscher et al.*, 2011]. Similarly, the minimum age of fresh water over the Gakkel Ridge is 3.4 yr, but with realistic scavenging rates this must be appreciably longer. ^{228}Ra distribution and ^{228}Th/^{228}Ra ingrowth give independent proof of the high age of the water in the eastern Eurasian basin over the Gakkel Ridge. We conclude that there must be a recirculation of shelf water in this basin (Figure 19), as this has been suggested in earlier studies of surface circulation [*Gordienko and Laktionov*, 1969]. This situation is very similar to the inferred recirculation of shelf water in the Canada Basin near the ICEX station [*Kadko and Muench*, 2005].
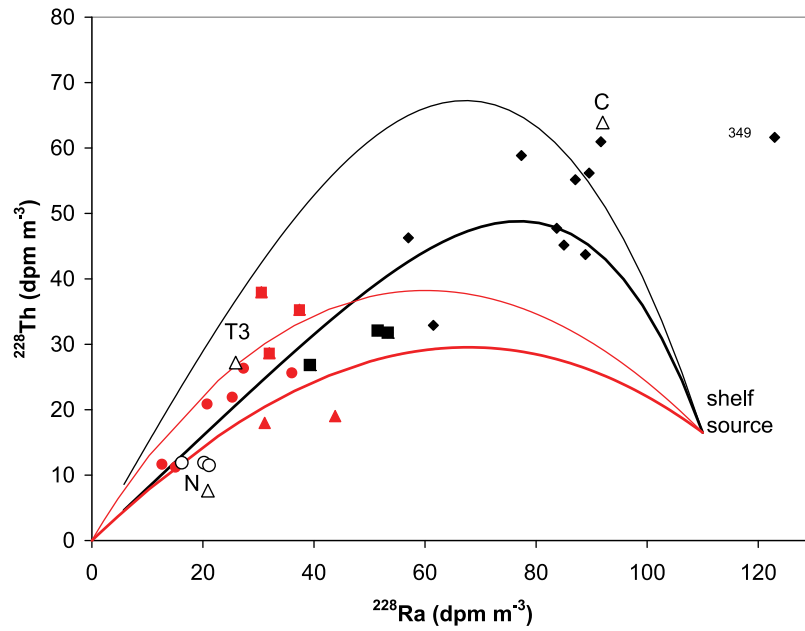
Figure 18. Thorium-228 versus [228]Ra in surface waters over the deep basins (symbols as in Figure 9) compared with model results for the mixing model (red lines) and the advection model (black lines) assuming a Th scavenging rate λ_s of 0 (thin lines) and 0.21 y^{-1} (heavy lines).
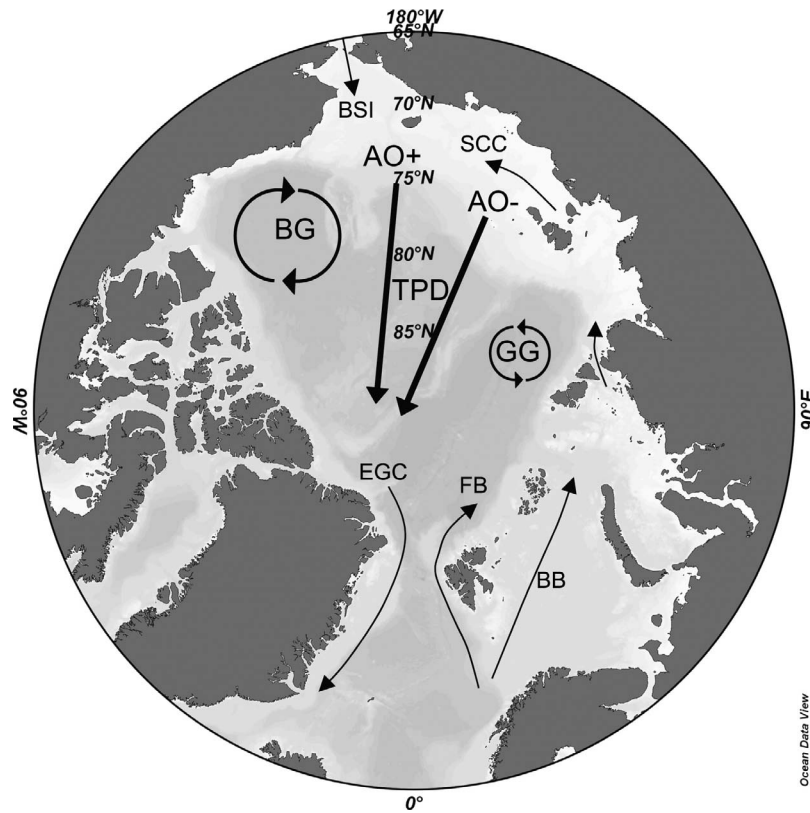

Figure 19. Conceptual graph of approximate location of TPD with highest [228]Ra concentrations during high (AO$^+$, as in early 1990s) and low (AO$^-$, as in 2007) Arctic Oscillation, the Beaufort Gyre (BG) and the inferred recirculation in the eastern Eurasian Basin (Gakkel Gyre (GG)) on a map based on *Rudels* [2009] with Bering Strait Inflow (BSI), Fram Strait (FB) and Barents Sea Branch (BB) of Atlantic inflow, Siberian Coastal Current (SCC), and East Greenland Current (EGC).

References

Abrahamsen, E. P., M. P. Meredith, K. K. Falkner, S. Torres-Valdes, M. J. Leng, M. B. Alkire, S. Bacon, S. W. Laxon, I. Polyakov, and V. Ivanov (2009), Tracer-derived freshwater composition of the Siberian continental shelf and slope following the extreme Arctic summer of 2007, *Geophys. Res. Lett.*, 36, L07602, doi:10.1029/2009GL037341.

Bacon, M. P., C.-A. Huh, and R. M. Moore (1989), Vertical profiles of some natural radionuclides over the Alpha Ridge, Arctic Ocean, *Earth Planet. Sci. Lett.*, 95, 15–22, doi:10.1016/0012-821X(89)90164-7.

Baskaran, M., D. J. Murphy, P. H. Santschi, J. C. Orr, and D. R. Schink (1993), A method for rapid in situ extraction and laboratory determination of Th, Pb, Ra isotopes from large volumes of seawater, *Deep Sea Res., Part I*, 40, 849–865, doi:10.1016/0967-0637(93)90075-E.

Baskaran, M., P. W. Swarzenski, and D. Porcelli (2003), Role of colloidal material in the removal of ^{234}Th in the Canada basin of the Arctic Ocean, *Deep Sea Res., Part I*, 50, 1353–1373, doi:10.1016/S0967-0637(03)00140-7.

Bauch, D., M. Rutgers van der Loeff, N. Andersen, K. Bakker, S. Torres-Valdes, and P. Abrahamsen (2011), Origin of freshwater and polynya water in the Arctic Ocean halocline in 2007, *Prog. Oceanogr.*, 91, 482–495, doi:10.1016/j.pocean.2011.07.017.

Broecker, W. S., A. Kaufman, and R. M. Trier (1973), The residence time of Thorium in surface seawater and its implications regarding the fate of reactive pollutants, *Earth Planet. Sci. Lett.*, 20, 35–44, doi:10.1016/0012-821X(73)90137-4.

Broecker, W. S., J. Goddard, and J. L. Sarmiento (1976), The distribution of ^{226}Ra in the Atlantic Ocean, *Earth Planet. Sci. Lett.*, 32, 220–235, doi:10.1016/0012-821X(76)90063-7.

Cai, P., M. Rutgers van der Loeff, I. Stimac, E.-M. Nöthig, K. Lepore, and S. B. Moran (2010), Low export flux of particulate organic carbon in the central Arctic Ocean as revealed by ^{234}Th:^{238}U disequilibrium, *J. Geophys. Res.*, 115, C10037, doi:10.1029/2009JC005595.

Chung, Y., and H. Craig (1980), ^{226}Ra in the Pacific Ocean, *Earth Planet. Sci. Lett.*, 49, 267–292, doi:10.1016/0012-821X(80)90072-2.

Cochran, J. K., D. J. Hirschberg, H. D. Livingston, K. O. Buesseler, and R. M. Key (1995), Natural and anthropogenic radionuclide distributions in the Nansen Basin, Arctic Ocean: Scavenging rates and circulation time scales, *Deep Sea Res., Part II*, 42, 1495–1517, doi:10.1016/0967-0645(95)00051-8.

Coppola, L., M. Roy-Barman, P. Wassmann, S. Mulsow, and C. Jeandel (2002), Calibration of sediment traps and particulate organic carbon using ^{234}Th in the Barents Sea, *Mar. Chem.*, 80, 11–26, doi:10.1016/S0304-4203(02)00071-3.

Cutter, G., P. Andersson, L. Codispoti, P. Croot, R. Francois, M. Lohan, H. Obata, and M. R. d. Loeff (2010), *Sampling and Sample-handling Protocols for GEOTRACES Cruises*, [electronic], GEOTRACES Stand. and Intercalibration Comm., Toulouse, France.

Ekwurzel, B., P. Schlosser, R. A. Mortlock, R. G. Fairbanks, and J. H. Swift (2001), River runoff, sea ice meltwater, and Pacific water distribution and mean residence times in the Arctic Ocean, *J. Geophys. Res.*, 106, 9075–9092, doi:10.1029/1999JC000024.

Elsinger, R. J., P. T. King, and W. S. Moore (1982), Radium-224 in natural waters measured by g ray spectrometry, *Anal. Chim. Acta*, 144, 277–281, doi:10.1016/S0003-2670(01)95545-X.

Frank, M. (1996), Spurenstoffuntersuchungen zur Zirkulation im eurasischen Becken des Nordpolarmeeres, Ph.D. dissertation, Ruprecht-Karls-Univ. Heidelberg, Heidelberg, Germany.

Garcia-Solsona, E., J. Garcia-Orellana, P. Masqué, and H. Dulaiova (2008), Uncertainties associated with ^{223}Ra and ^{224}Ra measurements in water via a Delayed Coincidence Counter (RaDeCC), *Mar. Chem.*, 109, 198–219, doi:10.1016/j.marchem.2007.11.006.

Geibert, W., M. Charette, G. Kim, W. S. Moore, J. Street, M. Young, and A. Paytan (2008), The release of dissolved actinium to the ocean: A global comparison of different end-members, *Mar. Chem.*, 109, 409–420, doi:10.1016/j.marchem.2007.07.005.

Gordienko, P. A., and A. F. Laktionov (1969), Circulation and physics of the Arctic Basin Waters, in *Annals of the International Geophysical Year, Oceanography*, edited by A. Gordon and F. W. G. Baker, pp. 94–112, Pergamon, New York.

Guay, C. K., and K. K. Falkner (1997), Barium as a tracer of Arctic halocline and river waters, *Deep Sea Res., Part II*, 44, 1543–1569, doi:10.1016/S0967-0645(97)00066-0.

Hansell, D. A., D. Kadko, and N. R. Bates (2004), Degradation of terrigenous dissolved organic carbon in the western Arctic Ocean, *Science*, 304, 858–861, doi:10.1126/science.1096175.

Jones, E. P., L. G. Anderson, and J. H. Swift (1998), Distribution of Atlantic and Pacific waters in the upper Arctic Ocean: Implications for circulation, *Geophys. Res. Lett.*, 25, 765–768, doi:10.1029/98GL00464.

Kadko, D., and K. Aagaard (2009), Glimpses of Arctic Ocean shelf-basin interaction from submarine-borne radium sampling, *Deep Sea Res., Part I*, 56, 32–40, doi:10.1016/j.dsr.2008.08.002.

Kadko, D., and R. Muench (2005), Evaluation of shelf-basin interaction in the western Arctic by use of short-lived radium isotopes: The importance of mesoscale processes, *Deep Sea Res., Part II*, 52, 3227–3244, doi:10.1016/j.dsr2.2005.10.008.

Kadko, D., R. S. Pickart, and J. Mathis (2008), Age characteristics of a shelf-break eddy in the western Arctic and implications for shelf-basin exchange, *J. Geophys. Res.*, 113, C02018, doi:10.1029/2007JC004429.

Kaufman, A., Y.-H. Li, and K. K. Turekian (1981), The removal rates of ^{234}Th and ^{228}Th from waters of the New York Bight, *Earth Planet. Sci. Lett.*, 54, 385–392, doi:10.1016/0012-821X(81)90054-6.

Key, R. M., W. S. Moore, and J. L. Sarmiento (1992), *Transient Tracers in the Ocean North Atlantic Study. Final Data Report for ^{228}Ra and ^{226}Ra*, 193 pp., Ocean Tracer Lab., Princeton, N. J.

Klunder, M. B., D. Bauch, P. Laan, H. J. W. de Baar, S. van Heuven, and S. Ober (2012), Dissolved iron in the Arctic shelf seas and surface waters of the central Arctic Ocean: Impact of Arctic river water and ice-melt, *J. Geophys. Res.*, 117, C01027, doi:10.1029/2011JC007133.

Lalande, C., K. Lepore, L. W. Cooper, J. M. Grebmeier, and S. B. Moran (2007), Export fluxes of particulate organic carbon in the Chukchi Sea: A comparative study using ^{234}Th/^{238}U disequilibria and drifting sediment traps, *Mar. Chem.*, 103, 185–196, doi:10.1016/j.marchem.2006.07.004.

Lalande, C., S. B. Moran, P. Wassmann, J. M. Grebmeier, and L. W. Cooper (2008), ^{234}Th-derived particulate organic carbon fluxes in the northern Barents Sea with comparison to drifting sediment trap fluxes, *J. Mar. Syst.*, 73, 103–113, doi:10.1016/j.jmarsys.2007.09.004.

Lepore, K., and B. Moran (2007), Seasonal changes in thorium scavenging and particle aggregation in the western Arctic Ocean, *Deep Sea Res., Part I*, 54, 919–938, doi:10.1016/j.dsr.2007.03.001.

Lepore, K., et al. (2007), Seasonal and interannual changes in particulate organic carbon export and deposition in the Chukchi Sea, *J. Geophys. Res.*, 112, C10024, doi:10.1029/2006JC003555.

Lepore, K., S. B. Moran, and J. N. Smith (2009), ^{210}Pb as a tracer of shelf-basin transport and sediment focusing in the Chukchi Sea, *Deep Sea Res., Part II*, 56, 1305–1315, doi:10.1016/j.dsr2.2008.10.021.

Letscher, R. T., D. A. Hansell, and D. Kadko (2011), Rapid removal of terrigenous dissolved organic carbon over the Eurasian shelves of the Arctic Ocean, *Mar. Chem.*, 123, 78–87, doi:10.1016/j.marchem.2010.10.002.

Li, Y.-H., H. W. Feely, and J. R. Toggweiler (1980), ^{228}Ra and ^{228}Th concentrations in GEOSECS Atlantic surface waters, *Deep Sea Res., Part A*, 27, 545–555.

McLaughlin, F. A., E. C. Carmack, R. W. Macdonald, and J. K. B. Bishop (1996), Physical and geochemical properties across the Atlantic/Pacific water mass front in the southern Canadian Basin, *J. Geophys. Res.*, 101, 1183–1197, doi:10.1029/95JC02634.

Middag, R., H. J. W. de Baar, P. Laan, and M. B. Klunder (2011), Fluvial and hydrothermal input of manganese into the Arctic Ocean, *Geochim. Cosmochim. Acta*, 75, 2393–2408, doi:10.1016/j.gca.2011.02.011.

Moore, R. M., and J. N. Smith (1986), Disequilibria between ^{226}Ra, ^{210}Pb and ^{210}Po in the Arctic Ocean and the implications for the chemical modification of the Pacific water inflow, *Earth Planet. Sci. Lett.*, 77, 285–292, doi:10.1016/0012-821X(86)90140-8.

Moore, W. S. (1984), Radium isotope measurements using germanium detectors, *Nucl. Instrum. Methods Phys. Res.*, 223, 407–411, doi:10.1016/0167-5087(84)90683-5.

Moore, W. S. (2008), Fifteen years experience in measuring ^{224}Ra and ^{223}Ra by delayed coincidence counting, *Mar. Chem.*, 109, 188, doi:10.1016/j.marchem.2007.06.015.

Moore, W. S., and R. Arnold (1996), Measurement of ^{223}Ra and ^{224}Ra in coastal waters using a delayed coincidence counter, *J. Geophys. Res.*, 101, 1321–1329, doi:10.1029/95JC03139.

Moore, W. S., J. L. Sarmiento, and R. M. Key (1986), Tracing the Amazon component of surface Atlantic water using ^{228}Ra, salinity and silica, *J. Geophys. Res.*, *91*, 2574–2580, doi:10.1029/JC091iC02p02574.

Moran, S. B., and J. N. Smith (2000), ^{234}Th as a tracer of scavenging and particle export in the Beaufort Sea, *Cont. Shelf Res.*, *20*, 153–167, doi:10.1016/S0278-4343(99)00065-5.

Moran, S. B., K. M. Ellis, and J. N. Smith (1997), ^{234}Th/^{238}U disequilibrium in the central Arctic Ocean: Implications for particulate organic carbon export, *Deep Sea Res., Part II*, *44*, 1593–1606, doi:10.1016/S0967-0645(97)00049-0.

Moran, S. B., et al. (2005), Seasonal changes in POC export flux in the Chukchi Sea and implications for water column-benthic coupling in Arctic shelves, *Deep Sea Res., Part II*, *52*, 3427–3451, doi:10.1016/j.dsr2.2005.09.011.

Morison, J., M. Steele, T. Kikuchi, K. Falkner, and W. Smethie (2006), Relaxation of central Arctic Ocean hydrography to pre-1990s climatology, *Geophys. Res. Lett.*, *33*, L17604, doi:10.1029/2006GL026826.

Östlund, G., and G. Hut (1984), Arctic Ocean water mass balance from isotope data, *J. Geophys. Res.*, *89*, 6373–6381, doi:10.1029/JC089iC04p06373.

Pfirman, S. L., R. Colony, D. Nürnberg, H. Eicken, and I. Rigor (1997), Reconstructing the origin and trajectory of drifting Arctic sea ice, *J. Geophys. Res.*, *102*, 12,575–12,586, doi:10.1029/96JC03980.

Pfirman, S., B. Tremblay, and C. Fowler (2009), Going with the Floe?, *Am. Sci.*, *97*, 484–493, doi:10.1511/2009.81.484.

Proshutinsky, A. Y., and M. A. Johnson (1997), Two circulation regimes of the wind-driven Arctic Ocean, *J. Geophys. Res.*, *102*, 12,493–12,514, doi:10.1029/97JC00738.

Rachor, E. (1997), *Scientific Cruise Report of the Arctic Expedition ARK-XI/1 of RV "Polarstern" in 1995*, 156 pp., Alfred Wegener Inst. for Polar and Mar. Res., Bremerhaven, Germany.

Roeske, T., D. Bauch, M. Rutgers v. d. Loeff, and B. Rabe (2012), Utility of dissolved Barium in distinguishing North American from Eurasian runoff in the Arctic Ocean, *Mar. Chem.*, in press.

Rudels, B. (2009), Ocean Current: Arctic Ocean Circulation, in *Encyclopedia of Ocean Sciences*, 2nd ed., edited by J. Steele, S. Thorpe, and K. Turekian, pp. 211–225, Elsevier, Boston, Mass., doi:10.1016/B978-012374473-9.00601-9.

Rutgers van der Loeff, M. M., R. M. Key, J. C. Scholten, D. Bauch, and A. Michel (1995), ^{228}Ra as a tracer for shelf water in the Arctic Ocean, *Deep Sea Res., Part II*, *42*, 1533–1553, doi:10.1016/0967-0645(95)00053-4.

Rutgers van der Loeff, M. M., R. Meyer, B. Rudels, and E. Rachor (2002), Resuspension and particle transport in the benthic nepheloid layer in and near Fram Strait in relation to faunal abundances and ^{234}Th depletion, *Deep Sea Res., Part I*, *49*, 1941–1958, doi:10.1016/S0967-0637(02)00113-9.

Rutgers van der Loeff, M. M., S. Kuhne, M. Wahsner, H. Holtzen, M. Frank, B. Ekwurzel, M. Mensch, and V. Rachold (2003), ^{228}Ra and ^{226}Ra in the Kara and Laptev seas, *Cont. Shelf Res.*, *23*, 113–124, doi:10.1016/S0278-4343(02)00169-3.

Rutgers van der Loeff, M. M., et al. (2006), A review of present techniques and methodological advances in analyzing ^{234}Th in aquatic systems, *Mar. Chem.*, *100*, 190–212, doi:10.1016/j.marchem.2005.10.012.

Rutgers van der Loeff, M. M., P. Cai, I. Stimac, A. Bracher, R. Middag, M. Klunder, and S. Van Heuven (2011), ^{234}Th in surface waters: Distribution of particle export flux across the Antarctic Circumpolar Current and in the Weddell Sea during the GEOTRACES expedition ZERO and DRAKE, *Deep Sea Res., Part II*, *58*, 2749–2766, doi:10.1016/j.dsr2.2011.02.004.

Schauer, U. (2008), The expedition ARKTIS-XXII/2 of the research vessel "Polarstern" in 2007, *Rep. Polar Mar. Res.*, *579*, 271 pp.

Schlosser, P., D. Bauch, R. Fairbanks, and G. Bönisch (1994), Arctic river run-off: Mean residence time on the shelves and in the halocline, *Deep Sea Res., Part I*, *41*, 1053–1068, doi:10.1016/0967-0637(94)90018-3.

Schlosser, P., R. Bayer, G. Bönisch, L. W. Cooper, B. Ekwurzel, W. J. Jenkins, S. Khatiwala, S. Pfirman, and W. M. Smethie (1999), Pathways and mean residence times of dissolved pollutants in the ocean derived from transient tracers and stable isotopes, *Sci. Total Environ.*, *237–238*, 15–30, doi:10.1016/S0048-9697(99)00121-7.

Serreze, M. C., A. Barrett, A. J. Slater, M. Steele, J. Zhang, and K. E. Trenberth (2006), The large-scale freshwater cycle in the Arctic, *J. Geophys. Res.*, *111*, C11010, doi:10.1029/2005JC003424.

Smith, J. N., S. B. Moran, and R. W. Macdonald (2003), Shelf-basin interactions in the Arctic Ocean based on ^{210}Pb and Ra isotope tracer distributions, *Deep Sea Res., Part I*, *50*, 397–416, doi:10.1016/S0967-0637(02)00166-8.

Trimble, S. M., and M. Baskaran (2005), The role of suspended particulate matter in ^{234}Th scavenging and ^{234}Th-derived export fluxes of POC in the Canada Basin of the Arctic Ocean, *Mar. Chem.*, *96*, 1–19, doi:10.1016/j.marchem.2004.10.003.

Trimble, S. M., M. Baskaran, and D. Porcelli (2004), Scavenging of thorium isotopes in the Canada Basin of the Arctic Ocean, *Earth Planet. Sci. Lett.*, *222*, 915–932, doi:10.1016/j.epsl.2004.03.027.

Walker, S. A., R. M. W. Amon, C. Stedmon, S. Duan, and P. Louchouarn (2009), The use of PARAFAC modeling to trace terrestrial dissolved organic matter and fingerprint water masses in coastal Canadian Arctic surface waters, *J. Geophys. Res.*, *114*, G00F06, doi:10.1029/2009JG000990.

Wassmann, P., T. Ratkova, I. Andreassen, M. Vernet, G. Pedersen, and F. Rey (1999), Spring bloom development in the marginal ice zone and the central Barents Sea, *Marine Ecol.*, *20*, 321–346, doi:10.1046/j.1439-0485.1999.2034081.x.

Wassmann, P. et al. (2004), Particulate organic carbon flux to the arctic ocean sea floor, in *The Organic Carbon Cycle in the Arctic Ocean*, edited by R. Stein and R. W. MacDonald, pp. 101–138, Springer, Berlin, doi:10.1007/978-3-642-18912-8_5.

Yamamoto-Kawai, M., F. A. McLaughlin, E. C. Carmack, S. Nishino, and K. Shimada (2008), Freshwater budget of the Canada Basin, Arctic Ocean, from salinity, δ^{18}O, and nutrients, *J. Geophys. Res.*, *113*, C01007, doi:10.1029/2006JC003858.

D. Bauch, Leibniz Institute of Marine Sciences at University Kiel (IFM-GEOMAR), Wischhofstr. 1-3, Kiel D-24148, Germany.

P. Cai, State Key Laboratory of Marine Environmental Science, Xiamen University, 422 Siming Nanlu, Xiamen 361005, China.

C. Hanfland, T. Roeske, M. Rutgers van der Loeff, and I. Stimac, Alfred Wegener Institute for Polar and Marine Research, PO Box 120161, Bremerhaven D-27570, Germany. (mloeff@awi.de)

S. B. Moran, Graduate School of Oceanography, University of Rhode Island, 215 S. Ferry Rd., Narragansett, RI 02882, USA.